

DUST FILTRATION BY PLANET-INDUCED GAP EDGES: IMPLICATIONS FOR TRANSITIONAL DISKS

ZHAOHUAN ZHU^{1,2}, RICHARD P. NELSON³, RUOBING DONG¹, CATHERINE ESPAILLAT⁴, AND LEE HARTMANN²
Draft version December 15, 2018

ABSTRACT

By carrying out two-dimensional two-fluid global simulations, we have studied the response of dust to gap formation by a single planet in the gaseous component of a protoplanetary disk - the so-called “dust filtration” mechanism. We have found that a gap opened by a giant planet at 20 AU in a $\alpha=0.01$, $\dot{M} = 10^{-8}M_{\odot} \text{ yr}^{-1}$ disk can effectively stop dust particles larger than 0.1 mm drifting inwards, leaving a sub-millimeter dust cavity/hole. However, smaller particles are difficult to filter by a planet-induced gap due to 1) dust diffusion, and 2) a high gas accretion velocity at the gap edge. Based on these simulations, an analytic model is derived to understand what size particles can be filtered by the planet-induced gap edge. We show that a dimensionless parameter T_s/α , which is the ratio between the dimensionless dust stopping time and the disk viscosity parameter, is important for the dust filtration process. Finally, with our updated understanding of dust filtration, we have computed Monte-Carlo radiative transfer models with variable dust size distributions to generate the spectral energy distributions (SEDs) of disks with gaps. By comparing with transitional disk observations (e.g. GM Aur), we have found that dust filtration alone has difficulties to deplete small particles sufficiently to explain the near-IR deficit of transitional disks, except under some extreme circumstances. The scenario of gap opening by multiple planets studied previously suffers the same difficulty. One possible solution is by invoking both dust filtration and dust growth in the inner disk. In this scenario, a planet induced gap filters large dust particles in the disk, and the remaining small dust particles passing to the inner disk can grow efficiently without replenishment from fragmentation of large grains. Predictions for ALMA have also been made based on all these scenarios. We conclude that dust filtration with planet(s) in the disk is a promising mechanism to explain submm observations of transitional disks but it may need to be combined with other processes (e.g. dust growth) to explain the near-IR deficit.

Subject headings: accretion disks, stars: formation, stars: pre-main sequence

1. INTRODUCTION

The transitional and pre-transitional disks are protoplanetary disks around young stars which exhibit strong dust emission at wavelengths $\gtrsim 10\mu\text{m}$, while showing significantly reduced fluxes relative to typical T Tauri disks at shorter wavelengths (e.g., Strom et al. 1989, Calvet et al. 2002, 2005; D’Alessio et al. 2005; Espaillat et al. 2007, 2008). Pre-transitional disks still have some infrared emission from warm, optically-thick dust near the star (Espaillat et al. 2007, 2008, 2010), while transitional disks only have near- and mid-infrared emission from optically-thin dust (Calvet et al. 2002, 2005; Espaillat et al. 2010). The depletion of near- to mid-infrared emission is generally interpreted as being due to evacuation of the disk interior to scales ~ 5 to ~ 50 AU (Marsh & Mahoney 1992; Calvet et al. 2002, 2005; Rice et al. 2003; Schneider et al. 2003; Espaillat et al. 2007, 2008, 2010; Hughes et al. 2009), an interpretation confirmed in some cases via direct sub-mm imaging (e.g., Pietu et al. 2006; Brown et al. 2007, 2009; Hughes et al. 2009; Andrews et al. 2009, 2011).

These cavities need to be both *large* and *deep* concern-

ing the dust surface density (e.g. Espaillat et al. 2010). Here *deep* means the gap is optically thin at mid-IR. In the case of the transitional disks, the optically-thin region must extend from radii as large as tens of AU all the way in to the central star, forming a dust hole. Even the pre-transitional disks, which display evidence of optically-thick dust emission in the innermost regions, must have large disk gaps from \sim AU scales to tens of AU. The requirement that the gaps/holes are optically thin implies that the population of dust in sizes of order a micron or less must be extremely small, due to the large opacity of these small dust grains.

Furthermore, many of these objects also exhibit gas accretion rates comparable to but slightly smaller than T Tauri disk accretion rates ($\sim 10^{-8}M_{\odot} \text{ yr}^{-1}$; Hartmann et al. 1998) onto their central stars (e.g. Calvet et al. 2002, 2005; Espaillat et al. 2007, 2008; Najita et al. 2007). Maintaining this accretion requires a significant mass reservoir in the inner disk. The conflict between the moderate disk accretion rate (which means a high gas surface density) and the near-infrared deficit (which means a low dust density) puts strong constraints on any theoretical attempts to explain these objects (Zhu et al. 2011).

In summary, there are three observational constraints for (pre)transitional disks: 1) A wide gap/hole extending over one order of magnitude in radii, 2) A deep gap/hole that is optically thin, and 3) a moderate gas accretion rate.

Electronic address: zhuhu@astro.princeton.edu, r.p.nelson@qmul.ac.uk, rdong@astro.princeton.edu, cespaillat@cfa.harvard.edu, lhartm@umich.edu

¹ Department of Astrophysical Sciences, 4 Ivy Lane, Peyton Hall, Princeton University, Princeton, NJ 08544

² Dept. of Astronomy, University of Michigan, 500 Church St., Ann Arbor, MI 48109

³ Astronomy Unit, Queen Mary University of London, Mile End Road, London E1 4NS UK

⁴ Center for Astrophysics, 60 Garden St., Cambridge, MA 02138

Gap opening by multiple giant planets (Zhu et al. 2011, Dodson-Robinson & Salyk 2011) has been proposed to explain the wide gaps in (pre)transitional disks. However, Zhu et al. (2011) also pointed out that even with four giant planets, the opened gap is not deep enough to explain transitional disks, unless there are massive giant planets close to the central star. Zhu et al. (2011) concluded that dust depletion/growth is still required in the inner disk to be consistent with observations. On the other hand, Dodson-Robinson & Salyk (2011) speculated that dust may be significantly confined in the spiral density wakes or streamers. Both of these works imply that dust dynamics may need to be considered along with the gas dynamics.

By considering dust dynamics independently, one promising mechanism to explain these wide and deep (dust) gaps/holes is dust filtration by the gap outer edge opened by planet(s) (Paardekooper & Mellema 2006, Rice et al. 2006). This mechanism is intrinsically due to the dust being a pressureless system, while the gas orbital dynamics is affected by the gas pressure. Dust particles orbit the central star at the Keplerian speed, but the gas rotates slightly faster or slower than this depending on the radial pressure gradient. In this case the dust particles feel either a headwind or tailwind from the gas and start drifting radially in the disk. The net effect is that dust particles tend to drift toward gas pressure maxima. Thus, at the outer edge of a planet-induced gap where the radial density/pressure gradient is positive, dust particles drift outwards, possibly overcoming their coupling to the inward gas accretion process. Dust particles will then stay at the gap outer edge while the gas flows through the gap. This process is called 'dust filtration' (Rice et al. 2006), and it depletes the disk interior to the radius of the planet-induced gap of dust, forming a dust-depleted inner cavity.

However, this filtration process sensitively depends on the pressure gradient at the planet-induced gap outer edge and it only operates for large particles whose drift velocities are significant. Small particles strongly coupled to the gas flow can still penetrate the planet-induced gap to the inner disk. More importantly, dust diffusion may significantly reduce the filtration efficiency even for the big particles (Ward 2009). Thus it is crucial to understand what sized particles can be filtered by a realistic planet-induced gap. In this paper, we will show only 0.1 mm particles and above can be filtered by a realistic gap if the disk viscosity parameter $\alpha=0.01$ and accretion rate $\dot{M} = 10^{-8}M_{\odot} \text{ yr}^{-1}$. This size limit may decrease to 0.01 mm if the planet is very massive and the disk is less turbulent accreting at a low accretion rate. Although this can explain the cavity from submm observations of transitional disks, it cannot explain the near-IR deficit of these disks, given that significant small dust is still present in the inner disk. However, on the other hand, if dust filtration is combined with dust growth in the disk, the near-IR deficit of transitional disks can be very well reproduced.

In §2, we introduce the two-dimensional two-fluid simulations. In §3, we construct a simpler one dimensional model. Our results are presented in §4. A short discussion is presented in §5. Various scenarios trying to ex-

plain transitional disks are tested with the Monte-Carlo radiative transfer model in §6, and conclusions are drawn in §7.

2. 2D 2-FLUID SIMULATIONS

2.1. Numerical Algorithms

2.1.1. Gas component

The gas disk evolution is simulated with FARGO (Masset 2000), a two-dimensional hydrodynamic code which utilizes a fixed grid in cylindrical polar coordinates (R, ϕ). FARGO uses finite differences to approximate derivatives, and the evolution equations are divided into source and transport steps, similar to those of ZEUS (Stone et al. 1992). However, an orbital advection scheme has been incorporated which reduces the numerical diffusivity and significantly increases the allowable timestep as limited by the Courant-Friedrichs-Lewy (CFL) condition. Thus FARGO enables us to study the interaction between the disk and embedded planets over a full viscous timescale for disks. The set-up of the gaseous disk and the planet is discussed in §2.4.1.

2.1.2. Dust component

Beyond the gas component, we have implemented an additional fluid in FARGO to simulate the dust's response to the gas. The dust is treated as a low pressure fluid and couples with the gas via drag terms. No feedback from the dust on the gas is simulated, since dust filtration normally takes place when the gas density dominates the dust density. However, this assumption may be violated under some circumstances as discussed in §5.4. The drift terms are added as an additional source step for the dust fluid

$$\frac{\partial v_{r,d}}{\partial t} = -\frac{v_{r,d} - v_{r,g}}{t_s}, \quad (1)$$

$$\frac{\partial v_{\theta,d}}{\partial t} = -\frac{v_{\theta,d} - v_{\theta,g}}{t_s}, \quad (2)$$

where all other terms/steps are the same as the gaseous fluid (Stone & Norman 1992). Since we will focus on dust particles with radii smaller than 1 mm⁵, these particles are in the Epstein regime (Whipple 1972, Weidenschilling 1977), so that the dust stopping time (Takeuchi & Lin, 2002) is

$$t_s = \frac{s\rho_p}{\rho_g v_T}, \quad (3)$$

where ρ_g is the gas density, s is the dust particle radius, ρ_p is the dust particle density (we chose $\rho_p=1 \text{ g cm}^{-3}$), $v_T=\sqrt{8/\pi}c_s$, and c_s is the gas sound speed. Considering the mean disk density is $\rho_g = \Sigma_g/\sqrt{2\pi}H$, it can also be written as

$$t_s = \frac{\pi s \rho_p}{2 \Sigma_g \Omega}. \quad (4)$$

⁵ With our disk parameters, the mean free path of the molecule is 0.1 mm at 0.1 AU and 5 m at 10 AU, which is larger than the dust size. At the very inner disk, where the mean free path is small and the particles are no longer in the Epstein regime, the viscous velocity dominates the drift velocity so that whether the particles are in the Epstein regime is no longer important.

In a dimensionless form the stopping time can be written as

$$T_s = t_s \Omega \quad (5)$$

where Ω is the Keplerian angular velocity.

When the dust stopping time is far shorter than the hydro time step, the drift terms become stiff. With an explicit method, the time step Δt needs to be smaller than both the stopping time t_s , and the hydro time step constraint δt in order to be numerically stable. However, t_s is very small with micron size particles, thus an implicit method is desired. Considering that the ZEUS/FARGO scheme is first order accurate in time, the first order implicit scheme is

$$v_{r,d}^{n+1} = v_{r,d}^n - \frac{v_{r,d}^n - v_{r,g}^n}{t_s + \Delta t} \Delta t, \quad (6)$$

where $n+1$ denotes the quantities at the new time step. Since the drift term is stiff, it may be helpful if we go to a higher order scheme. It turns out that the second order scheme just requires replacing the Δt in the denominator with $\Delta t/2$.

Although the implicit method ensures a stable scheme no matter what the time step we use, Equation 6 suggests it merely adds Δt to the stopping time. The new equivalent stopping time is $\Delta t + t_s$ which can be significantly larger than the real t_s if the numerical time step is much larger than t_s . Thus in order to accurately study the dust drift which is controlled by t_s , the hydro time step needs to be comparable to t_s . By numerical testing we found that the radial drift velocity is close to the theoretical value only if the time step is close to t_s . We tried different schemes as mentioned above, but they differ little. Thus, to simulate the dynamics of dust particles much smaller than 1 mm correctly, the time step is set by the dust stopping time and is inversely proportional to the particle size. Simulating dust drift for 0.01 mm particles is thus very computationally expensive since it is 100 times more expensive than simulating 1 mm particles.

On the other hand, we are not interested in dust dynamics happening on the dust stopping timescale. We are only interested in the dust's final response to the gas flow which changes on a much longer timescale than the stopping time. In other words, we can use the dust's terminal velocity to represent its final response to the gas. This is introduced as the ‘‘Short Friction Time Approximation’’ (SFT) in Johansen & Klahr (2005), where the dust velocity is related with the gas velocity as

$$\mathbf{v}_d = \mathbf{v}_g + t_s \frac{\nabla P}{\rho}. \quad (7)$$

This approximation is valid only if t_s is much smaller than the dynamical timescale of the gas flow. More accurately, t_s needs to be smaller than the hydrodynamic time step. In our simulation set-up, even with 1mm particles, t_s is at least one order of magnitude smaller than the hydrodynamic time step. In the Appendix we compare the SFT approximation with the two-fluid simulation and show good agreement between them.

Furthermore, dust can diffuse in the gaseous disk due to turbulence. In this work dust diffusion is implemented in the operator split fashion in the source step for the

dust fluid

$$\frac{\partial \Sigma_d}{\partial t} = -\nabla \cdot \left(D \Sigma_g \nabla \left(\frac{\Sigma_d}{\Sigma_g} \right) \right), \quad (8)$$

where D is the turbulent diffusivity which relates with the turbulent viscosity ν through

$$D = \frac{\nu}{Sc}, \quad (9)$$

where Sc is the Schmidt number defined as the ratio between the total accretion stress and particle mass diffusivity. Note that ν here is the viscosity of the ‘gaseous’ disk, representing the efficiency of the angular momentum transport experienced by the gas disk due to dust turbulence. When the disk orbital time (which is close to the turbulent eddy turnover time) is much larger than the dust stopping time (which is always true for particles smaller than ~ 1 mm), $Sc \sim 1$ (Johansen & Klahr 2005, Carballido et al. 2011) and dust will not settle significantly so that 2-D approximation is better justified. The above formula for dust diffusion has been confirmed by both analytic work and numerical simulations including both MRI turbulence and particle dynamics under the circumstances that the background gas surface density is uniform (Youdin & Lithwick 2007, Carballido et al. 2011). In §4, we discuss how diffusion plays a significant role in the dust filtration process.

2.2. Inner Boundary Conditions

For the gaseous fluid, as discussed by Crida, Morbidelli, & Masset (2007), a standard open inner boundary condition (Stone et al. 1992) in a fixed 2D grid can produce an unphysically rapid depletion of material through the inner boundary in the presence of the planets. There are two reasons for this. First, due to waves excited by the planet, the gas in the disk can have periodic inward and outward radial velocities larger than the net viscous velocity of accreting material. Thus, with the normal open boundary, material can flow inward while there is no compensating outflow allowed. Second, the orbit of the gas at the inner boundary is not circular due to the gravitational potential of the planets; again, as material cannot pass back out through the inner boundary, rapid depletion of the inner disk material is enhanced. As we are interested in the amount of gas depletion in the disk inward of the planet-induced gap(s) over substantial evolutionary timescales, it is important to avoid or minimize this unphysical mass depletion.

Crida et al. (2007) were able to ameliorate this problem by surrounding the 2D grid by extended 1D grids (FARGO2D1D, see their Figure 5). We follow Pierens & Nelson (2008), who found reasonable agreement with the Crida et al. results while using a 2D grid only by limiting the inflow velocities at the inner boundary to be no more than 3 times larger than the viscous radial velocity in a steady state,

$$v_{rs} = -\frac{3\nu_{in}}{2R_{in}}, \quad (10)$$

where ν_{in} and R_{in} are the viscosity and radius at the inner boundary. This scheme shows good agreement with the analytic estimate and the results from FARGO2D1D model (Pierens & Nelson 2008, Zhu et al. 2011).

For the dust fluid, we adopt a similar approach by limiting the radial velocity of the dust fluid to be no more than 3 times larger than the dust drift speed in a viscous disk,

$$v_{r,s,d} = \frac{-(3\nu_{in}/2R_{in})T_s^{-1} - \eta v_K}{T_s + T_s^{-1}}, \quad (11)$$

where η is the ratio between the pressure gradient and gravitational force $\eta = -(R\Omega^2\rho_g)^{-1}\partial P/\partial R$, and it is equal to $3/2(H/R)^2$ in our set-up below.

2.3. Fluids with and without pressure

A zero pressure fluid means zero scale height, which implies any velocity disturbance in the disk will quickly sharpen and shock, known as the delta shock⁶. In reality, a shock won't form in the particle fluid if there is a strong coupling between gas and dust. Numerically due to the inability to simulate coupling on scales smaller than the grid, a zigzag shaped density profile forms grid by grid in our simulations and we rely on the artificial viscosity to stabilize the shock. To minimize this effect, a small pressure is applied to the dust fluid here, which makes the scheme robust but it also introduces limitations as described below.

After numerical tests, we chose the dust scale height $H_d/R=0.0044$ for the dust fluid, which is one order of magnitude smaller than the gaseous fluid ($H/R=0.044$). H_d is close to our grid spacing, while significantly smaller than the gas disk scale height. Since dust drift is intrinsically due to the gaseous disk pressure gradient, adding 10% pressure to the dust fluid means the drift speed is only affected by 10%. But if the dust fluid has a sudden density change (e.g. 10 times steeper than the gaseous fluid) the effect of the small pressure can be amplified and becomes erroneous.

2.4. Model set-up

2.4.1. Gas component

Similar to Zhu et al. (2011), we assume a central stellar mass of $1M_\odot$ and a fully viscous disk. We further assume a radial temperature distribution $T = 221(R/AU)^{-1/2}$ K, which is roughly consistent with typical T Tauri disks in which irradiation from the central star dominates the disk temperature distribution (e.g., D'Alessio et al. 2001). The disk is vertically isothermal. The adopted radial temperature distribution corresponds to an implicit ratio of disk scale height to cylindrical radius $H/R = 0.029(R/AU)^{0.25}$. This differs from the $H/R = \text{constant}$ assumption used in many previous simulations, which implies a temperature distribution $T \propto R^{-1}$, which is inconsistent with observations. Consequently, our assumed temperature distribution with a constant viscosity parameter α ($\nu = \alpha c_s^2/\Omega$, where ν is the kinematic viscosity, c_s is the sound speed, Ω is the angular velocity) leads to a steady-disk surface density distribution $\Sigma \propto R^{-1}$ instead of the $\Sigma \propto R^{-1/2}$ which would result from either assuming both H/R and \dot{M} are constant, or both ν and viscous torque ($-2\pi R\Sigma\nu R^2 d\Omega/dR$)

⁶ If a delta shock forms in the disk, the fluid treatment needs to be replaced by a particle treatment since particles will cross orbits changing their distribution function in phase space.

are constant. This makes a significant difference in the innermost disk surface densities, and thus the implied inner disk optical depths in our models will be larger.

We set $\alpha = 0.01$ for the standard cases. Given our assumed disk temperature distribution, we set the initial disk surface density to be $\Sigma=178 (R/AU)^{-1}\exp(-R/100 \text{ AU}) \text{ g cm}^{-2}$ from $R \sim 8 - 300 \text{ AU}$, which yields a steady disk solution with an accretion rate $\dot{M} \sim 10^{-8}M_\odot \text{ yr}^{-1}$, typical of T Tauri disks (Gullbring et al. 1998; Hartmann et al. 1998).

2.4.2. Dust component

The dust surface density is assumed to be 0.01 of the gas surface density initially. With this set up, the dust stopping time $t_s \propto 1/(\Sigma_g\Omega) \propto R^{5/2}$. Motivated by (pre-)transitional disk observations, we place the planet at 20 AU.

We have carried out two-fluid simulations, with a $1 M_J$ planet in the gaseous and dust disk (1 mm particles) to 2.5×10^4 years, using two methods for the dust fluid: 1) self-consistently solving the dust fluid equations together with the gas equations, or 2) using the SFT approximation (Equation 7). In the following we will refer to the former as two-fluid simulations, and the second method as the SFT approximation (although the second method is also a two-fluid method). Good agreement has been found between these two methods (see Appendix). Since the SFT approximation is not limited by the dust stopping time, we use this approximation for the dust component in all the other runs.

Finally, gaseous and dust disks including three different size particles (1, 0.1, and 0.03 mm) and three different mass planets (1, 3, 6 M_J) have been simulated, respectively. All the runs are summarized in Tabel 1 and discussed in §4.3.

3. 1 D SIMULATION

Because the dust filtration process is mainly determined by the planet-induced gap structure which is quite axisymmetric except in the region close to the planet, it is useful to construct simpler azimuthally averaged 1-D models; by comparing 1-D models with 2-D simulations, we can separate effects due to axisymmetric and non-axisymmetric features. For axisymmetric flows, the dust surface density evolution is governed by the continuity equation (Takeuchi & Lin 2002)

$$\frac{\partial \Sigma_d}{\partial t} + \frac{1}{R} \frac{\partial}{\partial R} [R(F_{diff} + \Sigma_d v_d)] = 0, \quad (12)$$

where F_{diff} is the dust mass flux due to diffusion,

$$F_{diff} = -D\Sigma_g \frac{\partial}{\partial R} \left(\frac{\Sigma_d}{\Sigma_g} \right), \quad (13)$$

and v_d is the dust radial velocity in the rest frame due to the gas-drag

$$v_d = \frac{v_g T_s^{-1} - \eta v_K}{T_s + T_s^{-1}}, \quad (14)$$

where T_s , η are defined above. When $T_s \ll 1$ the above equation can be approximated by

$$v_d = v_g - \eta v_K T_s. \quad (15)$$

We can also incorporate the diffusion term in Equation 12 into the dust velocity so that the equivalent total dust velocity is

$$v_{d,t} = v_g - \eta v_K T_s - \frac{D}{R} \frac{d \ln(\Sigma_d / \Sigma_g)}{d \ln R}, \quad (16)$$

where the first term on the right hand side is the dust radial velocity induced by the gas radial velocity (normally it is negative due to the accretion process), the second term is the dust drift velocity with respect to the gas due to the gas pressure gradient (at the gap outer edge η is negative), and the last term is the dust velocity due to dust diffusion. The addition of the first two terms is the dust drift velocity in the rest frame without diffusion.

The only quantities which cannot be calculated in the 1-D models are the gaseous disk surface density with a gap opened by a planet (Σ_g , which is needed to calculate η) and the gas radial velocity v_g . Here, we adopt the gaseous disk surface density (Σ_g) from 2-D simulations, and the initial dust surface density is chosen as 1/100th of the gas surface density. We also assume the gas radial mass flux at each radius is a constant (equal to \dot{M}), giving

$$v_g = \frac{\dot{M}}{2\pi R \Sigma_g}. \quad (17)$$

This implies the gas velocity can be quite large deep inside the gap where the gas surface density is very low. This high velocity has significant impact on the dust drift as discussed in Rice et al. (2006) and §4.3. In 1-D, the radial velocity advection is ignored and the azimuthal velocity is assumed to be Keplerian. Thus we can simulate the pressureless fluid without worrying about shock formation. Furthermore, in our set-up, v_g and Σ_g are fixed, so that v_d is also fixed and the part of Equation 12 without diffusion is a linear equation for Σ_d . Due to the simplicity of the 1-D model, it not only extracts the essential physics but can also serve as a sanity check for 2-D simulations.

4. RESULTS

Before we present any results, we want to emphasize that Equation 16 guides all our discussions below. Dust filtration happens when Equation 16 (or Equation 15 if there is no dust diffusion) becomes positive so that the total dust velocity is outwards. In the following, we will first present the simplest case without dust diffusion and then we will present results with dust diffusion considered.

4.1. Dust Filtration without Diffusion

Although a 1 M_J planet can only open a shallow gap in the gas disk in our set-up, 1 mm dust particles can be effectively trapped at the gap outer edge. As shown in the left panel of Figure 1, the gaseous gap is barely apparent and the depth of the gap is half of the unperturbed disk. However, if dust diffusion is ignored, such a shallow gaseous gap can effectively stop 1 mm particles at the gap outer edge due to the dust drift. Then without replenishment, 1 mm dust particles in the inner disk quickly move inward to the central star, leaving a large mm dust cavity/hole in the disk (the second to left panel of Figure 1). The cavity is highly depleted by

four orders of magnitude. Thus the planetary wake is less apparent within the cavity, but it can still be seen outside the cavity. One feature which can be seen but is not very apparent in the dust image is the dust ring in the horseshoe region (the ring can also be observed in Figure 3). The ring forms because the gas pressure has a local maximum in the center of the horseshoe region, effectively trapping dust particles.

On the other hand, smaller particles (0.1 mm, the second to right panel) can still penetrate the planet-induced gap to the inner disk. This is because, without dust diffusion, the dust outward drift velocity with respect to the gas (the second term in Eq 15) decreases as T_s decreases and becomes comparable to the inward gas speed (the first term in Eq 15) so that the total dust velocity can be inward towards the central star. Since T_s is proportional to the particle size, it means smaller particles may not have enough outward drift to counteract the global accretion speed and they will be carried inwards across the gap by the gas, although at a small speed. This small speed, which implies a low dust accretion rate, can lead to the particles piling up at the outer edge of the gap. Thus the dust concentration is slightly increased at the outer edge of the gap, which makes the gap look deeper. But generally, the spatial structure of the small dust particles looks similar to that of the gaseous disk without a highly depleted cavity/hole.

For smaller particles (eg. 0.03 mm in the right-most panel of Figure 1), T_s decreases, and the dust disk behaves more similarly to the gaseous disk. In the extreme limit that dust particles are very small so that the drift velocity is negligible compared with the accretion velocity, the structure of the dust disk looks exactly like that of the gaseous disk.

4.2. Dust Filtration with Diffusion

The dust filtration process can be significantly hindered by dust diffusion, as originally pointed out by Ward (2009).

Dust diffusion tries to smooth any density feature of the dust relative to the gas. Thus, at the gap outer edge, dust tries to diffuse inwards, leading to an additional inward dust speed (adding the third term in Equation 16), which lowers the outward drift speed. The diffusion velocity (Eq 12) is

$$v_{diff} = -\frac{D}{R} \frac{d \ln(\Sigma_d / \Sigma_g)}{d \ln R}. \quad (18)$$

Unlike the gas diffusion velocity

$$v_g = -\frac{3}{R^{1/2} \Sigma_g} \frac{d}{dR} \left(R^{1/2} \nu \Sigma_g \right), \quad (19)$$

which depends on the gas surface density, the dust diffusion velocity depends on the dust concentration relative to the gas rather than on its absolute abundance.

At the beginning of the simulation, the abundances of dust and gas do not vary much so that the concentration of dust $\Sigma_d / \Sigma_g \sim 0.01$ everywhere and dust diffusion can be ignored. However, as shown in the last section, the dust quickly concentrates at the gap outer edge and dust diffusion can play a significant role. The timescale for dust diffusion becoming important is the dust radial drift timescale, assuming the gaseous disk is in steady

state,

$$\tau_{dust} = \frac{R_{gap}}{v_d} \quad (20)$$

where R_{gap} is the position of the planet-induced gap and v_d is defined in Equation 14. With our disk parameters ($\dot{M}=10^{-8}M_{\odot}\text{yr}^{-1}$, $\alpha=0.01$, $R_{gap}=20$ AU), $\tau_{dust}=9\times 10^4$ yr for 1 mm particles, 2×10^5 yr (the gas viscous timescale) for 0.1 mm and smaller particles. Thus, to study dust filtration, we have to evolve the disk long enough. For small dust particles (≤ 0.1 mm), it means to simulate the disk evolution at the disk viscous timescale at the position of the gap ($\sim 2\times 10^5$ yr). In this work, we managed to carry out such simulations by using the SFT approximation.

Figure 2 shows that dust diffusion significantly hinders dust filtration. Compared with the right panels of Figure 1, the dust gap is much shallower and the dust distribution is a lot smoother. 1 mm dust particles can still penetrate the gap opened by a 1 M_J planet, unlike the case without diffusion. However, dust diffusion cannot stop dust filtration indefinitely. If the gap is steeper (e.g. a gap opened by a 3 M_J planet, the lower panels of Figure 2), 1 mm dust particles can still be filtered by the gap, which will be discussed below.

4.2.1. Varying Gap Structure and Dust Sizes

Figure 3 shows both gas and dust surface density profiles for various planets in the disk (1, 3, 6 M_J from top to bottom) with and without dust diffusion (right and left panels, respectively). The solid curves are the gas surface densities divided by 100. At the end of the simulation, if the dust surface density is depleted by more than 1000 at the inner boundary (3 orders of magnitude smaller than the solid curve), we say the dust is significantly depleted and filtered.

The top panels show the disk surface densities with a 1 M_J planet at 20 AU. As discussed above, the gaseous gap is quite shallow, approximately half of the unperturbed disk surface density. Without dust diffusion, such a shallow gap is capable of filtering 1 mm dust particles, but unable to filter smaller particles. However, with dust diffusion, all the dust particle sizes we considered ($0.03 \leq s \leq 1$ mm) can pass through this 1 M_J planet-induced gap. Dust diffusion also changes the dust distribution in the outer disk: dust can diffuse outwards, slowing down the shrinkage of the dust disk and making the decline of the dust surface density with increasing radius more gradual.

The middle panels show the disk surface densities with a 3 M_J planet at 20 AU. The gaseous gap is one order of magnitude deep. Without dust diffusion, both 1 mm and 0.1 mm particles are filtered, while 0.03 mm particles can pass through. With dust diffusion, 1 mm particles are filtered, while 0.1mm and 0.03 mm particles pass through.

The lower panels show the disk surface densities with a 6 M_J planet at 20 AU. The gaseous gap is almost two orders of magnitude deep. Without dust diffusion, all kinds of particles are filtered. With dust diffusion, 1 mm and 0.1 mm particles are filtered.

To emphasize the effect of dust diffusion we use the simplest 1-D model to show various components of the dust velocity in Figure 4 for 1 mm particles in a gaseous disk with 1 M_J mass planet. The left panel shows the

case without dust diffusion, while the right panel includes dust diffusion. The gas velocity is the green curve. The total dust velocity is the solid black curve, including the dust drift velocity in the rest frame (the addition of the first and second terms of Equation 16, dotted curve) and the diffusion velocity (the third term of Equation 16, dashed curve). As shown in this figure, dust drift is fully capable of filtering the 1mm particles (the dust drift velocity in the rest frame is positive at the gap outer edge). However dust diffusion adds an additional negative velocity component. The net effect is that the total dust velocity is still inwards (dust filtration fails) when dust diffusion is considered.

In summary, dust diffusion hinders the dust filtration process. 1 mm-sized particles will be filtered by a gap one order of magnitude deep and particles with sizes ≥ 0.1 mm will be filtered by a gap that is two orders of magnitude deep.

4.3. High Gas Velocity at the Gap Edge

Another effect hindering filtration is the high gas velocity at the gap edge. Although this effect is self-consistently treated in simulations, it needs special attention in analytical approaches as noted in Rice et al. (2006). We have identified and verified this effect in our simulations.

Considering the gas accretion rate is constant across the planet-induced gap (if we allow the planet to accrete, this is still true at the outer edge of the gap), the radial velocity has to increase in the gap since the disk surface density decreases in the gap (according to $\dot{M} = 2\pi R\Sigma_g v_g$). With a two orders of magnitude deep gaseous gap, the gas velocity can be amplified by two orders of magnitude within the gap. Thus the first term of Equation 16 is significantly increased. Please note that this argument is built on the assumption that the velocity is axisymmetric inside the planet-induced gap. Although this assumption is incorrect deep inside the gap around the horseshoe orbits (see Appendix), the flow is quite axisymmetric at the edge of the gap where dust filtration takes place. We have checked 2-D simulations directly and confirmed that the radial velocity increases by a factor that is close to the gaseous gap depletion factor. This effect becomes increasingly important for a deeper gaseous gap.

To illustrate this effect, we again use the simplest 1-D model to show various components of the dust velocity, as shown in Figure 5. Even with dust diffusion considered, by ignoring the amplification of the gas radial velocity across the gap (green curve in the left panel is flat), 0.03 mm particles will be filtered in the 6 M_J gap. However, considering the gas velocity is amplified (the right panel), 0.03 mm particles can pass through the gap, consistent with the results from 2-D simulations.

4.4. What size particles will be filtered? Analytical approach

Although our simulations have suggested that 1 mm particles will be filtered by a gap one order of magnitude deep and ≥ 0.1 mm particles will be filtered by a gap that is two orders of magnitude deep, it would be insightful to have a simple analytic model to show how the critical filtration particle size depends on the disk parameters.

Both dust diffusion and high gas velocity at the gap edge are important as pointed out above. Thus we will consider them separately and then combine their effects.

First, we will assume the radial gas flow velocity is zero, and only consider the dust diffusion process to balance the dust drift. We are trying to find the marginal state between the dust being filtered and drifting inwards. This marginal state can be derived by assuming the diffusion velocity Equation 18 balances the drift velocity

$$-\nu \frac{d \ln(\Sigma_d/\Sigma_g)}{dR} = \frac{\eta V_K}{T_s + T_s^{-1}}. \quad (21)$$

Since $T_s \ll 1$, and plugging in $\eta = -(R\Omega^2\Sigma_g)^{-1}\partial P/\partial R$ and $\nu = \alpha c_s^2/\Omega$, we derive

$$\frac{d \ln(\Sigma_d/\Sigma_g)}{dR} = \frac{T_s}{\alpha} \frac{\partial \ln \Sigma_g}{\partial R}. \quad (22)$$

Here we have assumed the sound speed varies slowly compared with Σ_g so that it can be treated as a constant, which is a good approximation at the gap edges.

In order to proceed, we need to assign a planet-induced gap shape Σ_g , which can be derived by balancing the planetary torque density and the gradient of the viscous torque (Ward 2009)

$$3\pi\nu R^2\Omega \frac{\partial \Sigma_g}{\partial R} = \mu^2 R^2 \Omega^2 \Sigma_g \frac{R}{x^4}, \quad (23)$$

where $\mu = M_p/M_*$, and $x = (R - R_p)/R_p$. Assuming R , Ω , and ν are constant (which is a good approximation in the gap region compared with the factor x^{-4}), this equation can be integrated to obtain the gap profile

$$\Sigma_g = \Sigma_{g,0} e^{-|W/x|^3}, \quad W = \left(\frac{\mu^2 R^2 \Omega}{9\pi\nu} \right)^{1/3}. \quad (24)$$

where $\Sigma_{g,0}$ is the ambient unperturbed disk surface density⁷.

Plugging Equation 24 into Equation 22 and noticing that $T_s = \rho_p s \pi / (2\Sigma_g)$, we obtain

$$\frac{d \ln(\Sigma_d/\Sigma_g)}{dR} = \frac{3(W/x)^4 \rho_p s \pi e^{|W/x|^3}}{2\Sigma_{g,0} \alpha R_P W}. \quad (25)$$

Note that T_s is also a function of Σ_g , suggesting that dust and gas are more decoupled within the gap. Integrating this equation with respect to x , and assigning $T_{s,0} = \rho_p s \pi / (2\Sigma_{g,0})$, we derive

$$-\frac{T_{s,0}}{\alpha} e^{|W/x|^3} = \ln \left(\frac{\Sigma_d/\Sigma_g}{\Sigma_{d,0}/\Sigma_{g,0}} \right) = \ln \left(\frac{\gamma}{\gamma_0} \right) \quad (26)$$

where γ is the dust to gas mass ratio, Σ_d/Σ_g , at position x within the gap.

Then, x/W can be translated back to Σ/Σ_0 with Equation 24, giving

$$-\frac{T_{s,0}}{\alpha} \left(\frac{\Sigma_g}{\Sigma_{g,0}} \right)^{-1} = \ln \left(\frac{\gamma}{\gamma_0} \right). \quad (27)$$

⁷ When a gap is opened, the planetary torque density also decreases. Assuming the torque density only depends on $\Sigma_{g,0}$, we have overestimated the torque density so that our gap shape is sharper than a real gap.

The relationship between the dust depletion factor in the gap (γ/γ_0 , the depletion of the dust/gas mass ratio inside the gap compared with that outside the gap) and the gaseous gap depth ($\Sigma_g/\Sigma_{g,0}$) is shown in Figure 6 with the assumption that $\alpha=0.01$ and $\dot{M} = 10^{-8}M_\odot \text{yr}^{-1}$. As in §4.3.2, if the dust depletion factor is smaller than 0.001, then we consider that the particles are filtered efficiently. From the hydrodynamic simulations, we know the gaseous gap opened by a planet that is a few times more massive than Jupiter is on the order of 0.01 of the unperturbed disk surface density (this is clearly shown in the bottom panel of Figure 3 where the gaseous gap opened by a 6 M_J planet is 2 orders of magnitude deep.). Thus, Figure 6 shows particles smaller than 100 μm will penetrate through such a planet-induced gap and not be filtered.

We note that, with a given gap depth and structure, the dust depletion within the gap only depends on one dimensionless parameter $T_{s,0}/\alpha$. Since $T_{s,0} = \rho_p s \pi / (2\Sigma_{g,0})$, this parameter is $\propto s / (\Sigma_{g,0} \alpha)$. Considering that the quantity $\Sigma_{g,0} \alpha$ is proportional to the disk mass accretion rate (\dot{M}), $T_{s,0}/\alpha$ depends only on the particle size over the disk accretion rate ($\propto s/\dot{M}$). The curve labeled with 10 μm in our Figure 6 assuming $\dot{M} = 10^{-8}M_\odot \text{yr}^{-1}$ can also represent 100 μm particles in a $\dot{M} = 10^{-7}M_\odot \text{yr}^{-1}$ disk or 1 μm particles in a $\dot{M} = 10^{-9}M_\odot \text{yr}^{-1}$ disk. Thus if the disk accretion rate is very low, smaller dust can be filtered. The reason can be directly seen from Equation 21. With the same Σ_g and T_s , smaller α means less dust diffusion so that the critical particle size for which diffusion balances outward drift decreases. One caution is that the gap density (Equation 24) diverges to infinity when $x = 0$ and in reality the gap density profile truncate at some radius x . Here we rely on numerical simulations to determine where the gap truncates and the depth of the gap (γ/γ_0).

Now we consider the second effect: amplified gas radial velocity at the gap edge. The particle drift velocity due to the pressure gradient (the second term of Equation 16) not only needs to be larger than the diffusion velocity as above, but also needs to counter the gas radial velocity (v_g) within the gap. Here we compare the dust radial drift velocity derived above with the gas radial velocity from the gas accretion. The dust drift velocity (the right side of Equation 21) at the gap outer edge (Equation 24) is

$$v_{drift} = -\eta V_K T_s = \frac{3c_s^2 T_{s,0} W^3}{R_p \Omega x^4} e^{|W/x|^3} \quad (28)$$

Considering the gas flow velocity v_g outside the gap gives $v_{g,0} = -3\nu/(2R)$, and the gas velocity is amplified by $v_g = v_{g,0} \times \Sigma_{g,0}/\Sigma_g$ at the gap edge to maintain a constant accretion rate, we derive

$$\left| \frac{v_{drift}}{v_g} \right| = 2 \frac{T_{s,0}}{\alpha} (W/x)^4 \frac{1}{W}. \quad (29)$$

Again we can relate W/x with the gaseous gap depth $\Sigma_g/\Sigma_{g,0}$ from Equation 24 and obtain

$$\left| \frac{v_{drift}}{v_g} \right| = 2 \frac{T_{s,0}}{\alpha} \left[\ln \left(\frac{\Sigma_g}{\Sigma_{g,0}} \right) \right]^{4/3} \frac{1}{W}. \quad (30)$$

This is plotted in Figure 7. When $|v_{drift}/v_g|$ is smaller than 1, dust can pass through the gap with the gas due to the amplified gas velocity. Thus with a gap that is two orders of magnitude deep, $10 \mu\text{m}$ particles can pass through the gap with the gas. Again the dimensionless parameter $T_{s,0}/\alpha$ is present in this analysis. Here lower α means lower radial velocity and easier particle filtering. But besides that, another dimensionless parameter W is also present, and W depends on α , μ , and R . At smaller radii, dust is easier to filter since the outward drift velocity is larger. For the fixed radii, the dependence of W on α is rather weak.

When $|v_{drift}/v_g| < 1$, more dust particles can penetrate the gap than that estimated by Equation 27 which just considers dust diffusion. Thus, when the amplified gas velocity is important, Fig 6 only shows the lower limit of the depletion factor (marked as the thin curves). On the other hand when the dust diffusion dominates, Fig 6 shows the exact value of the dust depletion factor (marked as the thick curves).

Overall, for a planet (several M_J) present at 20 AU in a disk with $\alpha=0.01$ and $\dot{M} = 10^{-8}M_\odot \text{ yr}^{-1}$, the gap outer edge can filter particles larger than 0.1 mm, but particles smaller than 0.1 mm can pass through the planet-induced gap freely. If \dot{M} can be lowered to $10^{-9}M_\odot \text{ yr}^{-1}$, this critical size can decrease to $\sim 0.01\text{mm}$.

5. DISCUSSION

5.1. Comparison with previous work

Paardekooper & Mellema (2006) have carried out two fluid simulations similar to our approach but using a conservative Godunov scheme to study the response of mm sized dust to the planet. They focus on the minimum planet mass to open a gap in the dust disk and find a $0.05 M_J$ planet can open a gap in the mm-sized dust component. A similar result was also found using three dimensional SPH simulations by Fouchet et al. (2007). This can be understood as the thermal mass (Gc_s^3/Ω) of a dust disk is significantly lower than that of the gaseous disk since the dust is a pressureless system. Dust diffusion is ignored in these studies. But if the relative density between the dust and gas has a large gradient across the gap, dust diffusion may play an important role to smear out any feature in the dust disk. Our work focuses on gap opening by more massive planets to study the effect of the gaseous gap edge on smaller grains which are essential for near-IR deficit of transitional disk systems.

This dust filtration process by the planet-induced gaseous gap outer edge was first studied by Rice et al. (2006) with an analytical approach and they concluded micron sized particles can be filtered by the planet-induced gap. In detail they suggested that a gap opened by a $5 M_J$ planet might be able to filter $1 \mu\text{m}$ particles and above. However, numerical simulations are difficult to carry out to verify this since small particles have very short stopping time which limits the numerical time step. In this work we use the SFT approximation which allows us to study this problem using numerical simulations. We have found that the critical size for dust filtration is larger than that estimated by Rice et al. (2006). In our simulations, the gap outer edge near a $6 M_J$ planet can only filter $100\mu\text{m}$ particles and above. The difference partly comes from a lower accretion rate in their models

(the discussion of the critical particle size on disk accretion rate is in §4.4). But more importantly, the difference is due to dust diffusion (Ward 2009).

The larger critical particle size for filtration poses challenges to explain transitional disks with dust filtration alone, as discussed in §6.

5.2. Steady state, feedback and outer disk

Without considering dust feedback and dust diffusion, the dust velocity is fully determined by the gas surface density (Equation 14). Thus, due to the lack of feedback between the dust concentration and its velocity, the dust disk cannot achieve a steady state. Dust will continue to pile up at the outer edge of the gap (e.g. the upper left panel of Fig. 3), and eventually dust feedback on the gas through drag forces becomes important there, as pointed out by Ward (2009).

However, with dust diffusion considered, the dust concentration can affect the dust velocity (Equation 15), and a steady state can be reached on the dust drift timescale. This leads to a smoother and lower dust surface density (e.g. the upper right panel of Fig. 3), which weakens the dust feedback. Furthermore, with smaller and smaller particles, dust diffusion is much more important than the dust drift velocity so that the dust surface density is smoothed even more. But if the dust settles to the midplane, dust feedback through drag forces might still be quite important there, and needs further study.

The dust disk steady state can be calculated by assuming the product of the dust velocity and density is a constant. At the outer disk and for 1 mm particles, dust drift and diffusion velocities are far larger than the gas velocity. Thus we can seek a solution for which the last two terms of Equation 16 balance each other. It can be easily derived that a gaseous disk surface density varying as $\Sigma_g \propto R^\beta$ requires the dust surface density to vary as $\Sigma_d \propto R^{2\beta-4.5}$ if outward diffusion balances inward drift. If $\beta=1$, $\Sigma_d \propto R^{-2.5}$, which is consistent with our simulations with dust diffusion at the outer disk (the left panels of Fig. 3). This property has important implications for submm observations in protoplanetary disks. It suggests the dust disk will not shrink indefinitely if there is dust diffusion and we can use the dust surface density structure to imply the gas surface density structure.

5.3. How much dust can be filtered by a gap in a protoplanetary disk?

Since our simulations have determined the critical dust size due to gap edge filtration, we can estimate the fraction of dust mass being filtered by the gap in a protoplanetary disk.

The exact mass fraction of dust larger than some size depends on the dust size distribution function $n(s) \propto s^{-\beta}$, where s is the dust size. Dust in the diffuse interstellar medium is thought to have a size distribution $\beta = 3.5$ from 0.005 to $1\mu\text{m}$ (Mathis, Rumpl & Nordsieck 1977). In protoplanetary disks, the size distribution function can be flatter, possibly due to dust growth, with $\beta = 2.5$ (D'Alessio et al. 2001). The total dust mass fraction for particles smaller than s_p is

$$\frac{m(s < s_p)}{m(\text{total})} = \frac{s_p^{4-\beta} - s_{\min}^{4-\beta}}{s_{\max}^{4-\beta} - s_{\min}^{4-\beta}} \quad (\text{if } \beta \neq 4), \quad (31)$$

where s_{max} and s_{min} are the maximum and minimum sizes of the dust with distribution $n(s) \propto s^{-\beta}$. If both s_{max} and s_p are far larger than s_{min} , this reduces to $(s_p/s_{max})^{4-\beta}$.

Our simulations above suggest only dust equal or larger than 0.01–0.1 mm can be filtered. Thus if we adopt $s_{max} = 1\text{mm}$ (D’Alessio et al. 2001), the dust smaller than 0.1 mm only accounts for 10% of the total dust mass with $\beta = 3$ or 1% of the total dust mass with $\beta = 2$, and dust smaller than 0.01 mm only accounts for 1% of the total dust mass with $\beta = 3$. Thus the dust mass fraction is decreased significantly it crosses the planet-induced gap. With only 1% dust mass passing through the gap, the dust to gas ratio within the gap decreases to 10^{-4} . However, since all the micron-sized dust grains can pass through the gap freely, the near-IR SED of the disk is hardly affected by the filtration process, which will be emphasized in §6.

6. TRANSITIONAL DISKS

As summarized in the introduction, (pre-)transitional disks have wide and deep gaps, and a moderate gas accretion rate onto the star. Gap opening by planet(s) is an intriguing possibility. To produce these wide and deep gaps with planets, two scenarios have been proposed: gap opening by multiple planets (e.g. Zhu et al. 2011, Dodson-Robinson & Salyk 2011) and dust filtration (Rice et al. 2006).

Since both gap opening by multiple planets (Zhu et al. 2011) and dust filtration (this work) hardly affect the micron sized particle distribution within AU scales, the near-IR SEDs of these disks should look similar to those of classical T-Tauri disks. Thus both scenarios can explain pre-transitional disk near-IR SEDs, especially for those having the same SED as classical T-Tauri disks (Andrews et al. 2011). However, both of the scenarios have difficulties in reproducing transitional disk SEDs which have strong near-IR deficits.

In the following we will use a Monte-Carlo radiative transfer model to demonstrate this difficulty with both 1) gap opening by multiple planets, 2) dust filtration, and provide one possible solution with 3) filtration+grain growth to reproduce the transitional disk GM Aur’s SED.

6.1. Monte-Carlo radiative transfer set-up

The Monte Carlo radiative transfer code was developed by Whitney et al. (2003a,b), Robitaille et al. (2006), and Whitney et al. (2012), while for the disk structure see Whitney et al. (2003b) for references. This entire disk is composed of two dust components: a thick disk with small (i.e., ISM-like μm -sized) grains, and a thin disk with large (mm-sized) grains. We use the standard ISM dust model for the small dust (Kim et al. 1994), and use Model 3 in Wood et al. (2002) for the large dust ($\beta=3$ with the maximum particle size 1 mm). Both disk components are isothermal in the vertical direction, and their respective scale heights h_{thin} and h_{thick} obey a simple power law $h \propto R^\Psi$, with h_{thin} fixed to be $0.2 \times h_{thick}$. The disk extends from the sublimation radius (self-consistently determined by the dust sublimation temperature) to 200AU.

To reproduce a classical T Tauri disk SED for comparison, we set-up a full disk model, where the gas surface

density profile is $\Sigma_R = \Sigma_0 \frac{R_c}{R} e^{-R/R_c}$ and R_c is the scaling length fixed to be 100 AU. This is the same as our hydrodynamic simulations. Dust mass is 1% of the disk mass. Among all the dust, 1% is in the small dust, while the rest is in the large dust, which is equivalent to saying that the small dust depletion and settling factor is 0.01. This choice is based on both our argument in §5.3 (if the dust distribution function is $n(s) \propto s^{-3}$ from submicron sizes to 1 mm, 99% of the dust will be in the grains larger than 0.01 mm), and observational constraints (Furlan et al. 2006). Note that this implies dust has already grown to mm sizes in the outer disk and the small dust is only 1% of the total dust mass. The full disk model has a total mass of 0.1 M_\odot , and a scale height profile with $H/R = 0.075$ at 100 AU and $\Psi=1.2$. The accretion rate is assumed to be $10^{-8}M_\odot \text{yr}^{-1}$. These are nominal values for a classical T Tauri disk, and they are consistent with our hydrodynamical simulations. Since we are trying to fit the SED of GM Aur, the central source is assumed to be a 5730 K pre-main star with radius 1.5 R_\odot and mass 1.2 M_\odot (Calvet et al. 2005) and the inclination angle of this system is 55 degrees.

The full disk’s SED is shown as the dotted curves in the bottom panels of Fig. 8. It produces a strong near-IR flux, similar to a classical T Tauri disk SED. In the following we will modify this model based on results from hydrodynamic simulations trying to reproduce transitional disk GM Aur’s SED (the red curves in Fig. 8).

6.2. Gap Opening by Multiple Planets?

To simulate gap opening by multiple planets, we cut a wide gap in the disk for both small and large dust (the left panel of Figure 8). In Zhu et al. (2011), with the same disk structure, using hydrodynamic simulations, we found that four giant planets can open a gap from 2 to 20 AU with the gap depth 1/1000 th of the unperturbed disk surface density. Thus here we cut the gap from 2 to 25 AU and both small and large dust surface density is decreased by a factor of 1000 compared with the unperturbed disk. The gap is clearly seen in the dust surface density contours in the left panels of Figure 8. However, the near-IR SED from the modeled disk with 4 planets produces an SED more similar to that of classical T Tauri disks, rather than transitional disks (the left bottom panel). This is because the inner disk within 2 AU is the same as a full disk.

This similar SED is not surprising, since previous work has already suggested the near-IR deficit of transitional disk requires small dust in the inner disk, on scales less than 1 AU, to be depleted by many orders of magnitude (Espaillat et al. 2010, Zhu et al. 2011). To be more specific, considering most transitional disks have accretion rates $\sim 10^{-8}M_\odot \text{yr}^{-1}$ onto the star, and using

$$\Sigma_g = \frac{\dot{M}}{3\pi\nu}, \quad (32)$$

Σ_g is 10^2g/cm^2 at 0.1 AU for $\alpha = 0.01$. Considering that the nominal opacity of ISM dust at 10 μm is $10 \text{cm}^2/\text{g}$, the optical depth at 0.1 AU is 10^3 . But SED modeling of transitional disks (e.g. GM Aur) require the disk to be optically thin at 0.1 AU (Calvet et al. 2005); thus the micron-sized dust, which contributes most to the near-

IR flux, needs to be depleted at least by three orders of magnitude. However, gap opening by multiple planets from 2-20 AU has little effect on the dust distribution within AU scales and thus it won't prevent the near-IR SED from being similar to a full disk model.

6.3. Dust Filtration by the Gap?

To simulate the effect of dust filtration, large dust is absent within 25 AU compared with the full disk model (the middle panel of Figure 8). All large dust is assumed to be filtered. However the small dust can pass the planet-induced gap and has the same distribution as a full disk (middle panels of Figure 8)⁸. Again, although the mid-IR SED changes a little bit due to the depletion of the large dust, the optical to near-IR SED looks similar to the full disk (the middle bottom panel) since small dust dominates the optical to near-IR opacity.

This demonstrates that although dust filtration is efficient at reducing the total dust mass, since most of the dust mass resides in large dust particles (§5.3), it has little effect on the near-IR SED since this is determined by the micron-sized particles which can not be filtered by the gap. Although Dodson-Robinson & Salyk (2011) speculated that dust can be trapped in the spiral wakes, trapping in spiral wakes is only a second order effect compared with the gap filtration, since the density wakes have far smoother density profiles than the gap edge. If the gap edge fails to trap micron sized particles, the density wakes won't be able to trap these particles. Our two fluid simulations (Figure 2 and 11) also do not show dust pile up in the density wakes.

However, under some extreme circumstances (e.g. $\dot{M} \leq 10^{-9} M_{\odot} \text{yr}^{-1}$, the presence of a $10 M_J$ planet), the critical filtration size may decrease to $10 \mu\text{m}$. With a flat dust size distribution (e.g. $\beta=2$ in §5.3), dust smaller than $10 \mu\text{m}$ could have a mass less than 10^{-4} of the total dust mass. Thus, after filtration, small dust could have a depletion factor equal to 10^{-4} , which is close to the small dust depletion factor (10^{-5}) required to explain the near-IR deficit of GM Aur⁹.

In Fig. 9, we have calculated two cases with a small ($< 10 \mu\text{m}$)/large ($> 10 \mu\text{m}$) dust mass ratio $\sim 10^{-5}$ at the outer disk and only small dust existing in the inner disk. As expected, the near-IR deficit can be well reproduced due to the tiny amount of small dust in the inner disk. However, due to the small optical depth of the outer disk (the abundance of small particles is very low, and large dust grains have settled to the midplane forming a dust layer whose thickness is only 20% of the gas disk), the mid-IR flux is very weak and unable to reproduce the IRS observations (dotted curve in Fig. 9). In order to reproduce the mid-IR flux, the large dust grains have to remain suspended in the atmosphere of the disk and not settle (maintaining the same thickness as the gaseous disk, shown by the dashed curve in Fig. 9).

The dashed curve in Fig. 9 suggests that is not impossible for dust filtration alone to explain GM Aur. But

⁸ We neglect the narrow gap opened by the planet in this calculation as it will not significantly affect the SED.

⁹ If the gas surface density is very low (e.g. 2gcm^{-3}) the dust depletion factor can be 10^{-3} for the disk to be optically thin (Salyk et al. 2007). In this case, a large disk viscosity parameter α is required to explain the observed gas accretion rates.

several conditions have to be met: 1) dust grows significantly in the outer disk (flat dust size distribution, and the small dust ($< 10 \mu\text{m}$) to big dust mass ratio is 10^{-5}); 2) a very massive planet forms in a disk with a low accretion rate; 3) large grains in the outer disk cannot settle. These conditions are not easy to satisfy since a normal T Tauri disk has a small dust depletion factor of 0.1-0.001, and large grains are settled to the midplane. Furthermore GM Aur has a disk mass accretion rate $10^{-8} M_{\odot} \text{yr}^{-1}$.

6.4. Filtration+Grain Growth

To reproduce the near-IR deficit of transitional disk SEDs it is essential to reduce the small dust ($\leq 0.01 \text{mm}$) abundance in the inner disk within AU scales. One solution is considering the growth of small dust particles after large particles are filtered by the planet-induced gap. Dust can grow quite rapidly in the inner disk. It may only take 10^3 yrs for dust particles to grow from sub-micron sizes to $1000 \mu\text{m}$ at 1 AU (e.g. models S3 and S4 in Dullemond & Dominik 2005). One way to stop the rapid dust growth is by collisional fragmentation (Dullemond & Dominik 2005, Dominik & Dullemond 2008), in which case large particles are shattered to replenish small dust grains. The growth and fragmentation maintains a quasi-stationary dust size distribution function. In disks with gaps, if 99% of the dust mass is filtered (only 1% of the dust mass resides in particles smaller than the critical filtration size 0.1mm as estimated above with $\beta = 2$) when the gas flow passes the planet-induced gap, the remaining 1% of small grains that manage to pass through to the inner disk can grow quite efficiently without replenishment from fragmentation of large particles. Although the dust growth time is 100 times longer than the timescale for a non-filtered disk (the dust growth time is inversely proportional to the dust abundance), it is still modestly shorter than the viscous timescale at 20 AU with $\alpha=0.01$. Eventually a new balance is made, and the quasi-stationary dust size distribution is established again. At this time, due to grain growth, the small dust is only 1% of the abundance that was present after it had passed through the planet's orbit location. In other words, small dust is depleted indirectly due to dust growth and the net depletion factor for small particles in the inner disk is 10^{-4} (1% after filtration \times 1% mass fraction in the new size distribution). Such a scenario of "double depletion" may explain transitional disks, but requires further study to place it on a firmer foundation.

To simulate this scenario we assume small dust grows in the inner disk and reestablish the dust size distribution after large particles are filtered by the planet-induced gap at 25 AU. This is illustrated in the right panels of Fig. 8. In the inner disk we assume the new dust size distribution has a small to large dust mass ratio 1:999. Since the total dust mass is decreased to 1% after dust filtration and this new distribution further reduces the small dust by a factor of 1000, the small dust is depleted by a factor of 10^5 , and the mass ratio of small dust to gas is 10^{-7} . This leads to an optically thin inner disk. The disk's SED fits the GM Aur SED quite well in the bottom right panel.

Note that in this scenario small particle growth is a gradual process. Although we deplete the dust in the inner disk uniformly for computational convenience (up-

per two panels in the right column of Fig. 8, or in other words we assume small particles grow instantaneously after they cross the gap); in reality the abundance for small particles may change gradually and join the outer disk abundance smoothly.

In this work we only put one planet in the disk to study dust filtration, because the dust filtration process does not sensitively depend on the number of the planets in the disk since most dust will be filtered by the outermost planet gap or the deepest gap. Thus most of our results can also be applied to the gap opened by multiple planets in the disk, which is complementary to Zhu et al. (2011). We note, however, that a multiple planet system may need to be invoked to dynamically clear planetesimals from the inner disk region as the presence of such bodies is likely to provide a source for small dust grains through their mutual collisions.

6.5. Observational implications for ALMA

Dust filtration has other observational implications besides SEDs. Dust filtration by the planet-induced gap differentiates various particles. Thus if we observe transitional disks at various wavelengths the gap/cavity should be more distinctive at longer wavelengths. Dust growth as argued above won't happen instantaneously as the flow passes through the planet-induced gap. Thus at shorter wavelengths, the cavity which is found by submm observations is less apparent or even disappears (e.g. Fig. 1). Andrews et al. (2011) notice that there are (pre-)transitional disks with classical T-Tauri disk SEDs but that show gaps in submm interferometry. More directly, recent Subaru observations have found a lot of (pre-)transitional disks that have submm cavities (Andrews et al. 2011) do not show cavities in near-IR scattered light images (Dong et al. 2012). Both of these findings seem to agree with the dust filtration scenario.

However, after the big grains are filtered, whether and how much small grains can grow is a difficult issue; it requires a dust evolutionary model combined with dust dynamics. The complexity of the problem is illustrated by, for example, Birnstiel et al. (2011) and references therein. In this work, based on transitional disk SEDs, we suggest that small dust needs to grow in the inner disk. This hypothesis can also be tested by ALMA. Figure 10 shows both big dust (larger than the critical filtration size) surface density and the $850 \mu\text{m}$ opacity in the filtration+grain growth scenario¹⁰. Both the large dust surface density and the submm opacity change at the gap edge due to dust filtration. The submm opacity decreases by a factor >100 at the gap edge, which is consistent with submm constraints from Andrews et al. (2011). Although the exact value in this plot is only applied to our particular model as in Figure 8, the trend that the submm opacity decreases at the gap edge and then increases inwards is a signature of the filtration+grain growth scenario, which can be tested by ALMA.

More generally, ALMA can test all the three scenarios above. For gap opening by multiple planets without dust filtration, both gas (probed by molecular lines) and dust (probed by dust continuum) inside the gap should be

equally depleted. If dust filtration is at work, the mm sized dust will be more depleted inside the gap than the gas. To test whether there is grain growth inside the gap, we can use multiple wavelength observations to see how the slope of the opacity changes.

ALMA can also test if the dust and gas have similar density profiles at the outer disk beyond the gap. Our simulations suggest that, combining dust drift and diffusion, the dust and gas surface density profiles in the outer disk can be quite different (§5.4). Although submm observations (Andrews et al. 2012) have indeed suggested that the dust disk is more compact than the gaseous disk, the different surface density slopes between the dust and gas disks predicted in §5.4 need to be tested by future ALMA observations. But we note that dust growth and fragmentation can potentially change this relationship (e.g. Birnstiel et al. 2012).

6.6. Other Possibilities

As illustrated above, the key ingredient to reproduce the GM Aur SED is reducing the abundance of micron sized dust particles by five orders of magnitude in the inner disk while maintaining a sufficient gas accretion. Due to the good coupling between micron sized particles and the gas, any theory only considering gap formation in a gaseous disk is not enough, such as photoevaporation, gap opening by planets, etc. Dust growth and settling have to be considered. Besides filtration combined with dust growth, there are several other possibilities:

The first alternative is purely dust growth. If dust can grow significantly in the inner disk to make the inner disk optically thin, it can explain GM Aur's SED. In this scenario it may suggest transitional disks are older than CTTS, which has not been suggested by observations. Furthermore, both SED fitting and sub-mm observations suggest the gap edge is very sharp, inconsistent with the pure dust growth model. However, with CARMA, Isella et al. (2012) have suggested LkCa 15 can be explained by the pure dust growth model. Thus, pure dust growth could still be a possible solution.

The second alternative is a large gas mass reservoir close to the central star with a wide and deep gap beyond. The wide and deep gap can be caused by a very massive planet (or even a star) or several planets so there is no accretion flow from the outer disk to the inner disk. The accretion onto the star is sustained by the mass reservoir close to the planet (e.g. a dead zone). However this mass reservoir needs to be very narrow or depleted in small dust to not produce too much near-IR flux.

The third alternative is the dust being held back by the radiation pressure (Chiang & Murray-Clay 2007). However, the efficiency of the radiation pressure is questioned by Dominik & Dullemond (2011).

The fourth alternative is planet gap opening in layered disks. The pros and cons of this model will be discussed in a forthcoming paper.

However, there is one challenge to all the scenarios trying to explain transitional disks with gap opening by planet(s) located at a few tens of AU from the central star. In the core-accretion scenario, the solid component in the inner disk is likely to have undergone significant growth to form planetesimals and planetary embryos within the time taken to form the putative planet at ~ 20 AU. These planetesimals should collide and con-

¹⁰ To calculate the opacity, we assume the gas surface density is unaffected by the presence of the planet. The gaseous disk is the same as a constant \dot{M} accretion disk.

tinuously regenerate small dust grains. As we have alluded to earlier in this paper, one way round this problem is to invoke the presence of multiple planets in the inner disk to clear these planetesimals. But this hypothesis clearly requires further investigation.

6.7. *Transitional VS. Pre-transitional Disks*

Dust filtration also suggests more massive planets can lead to stronger dust filtration and depletion. Thus transitional disks may have higher mass planet(s) than pre-transitional disks. Since a higher mass planet exerts a stronger torque on the outer disk, it may slow down the accretion flow passing the planet and lead to a lower disk accretion rate onto the star. This is consistent with observations that transitional disks have lower accretion rates than pre-transitional disks (Espaillat et al. 2012).

Regarding dust growth, transitional disks put strict constraints on the dust abundance in the inner disk since the dust is optically thin. For pre-transitional disks, the dust abundance in the inner disk is difficult to constrain since it is optically thick. Thus it's possible to explain pre-transitional disks without invoking dust growth (e.g. dust filtration, multiple-planets, photoevaporation Alexander & Armitage 2007). However it's also possible that the planet(s) in pre-transitional disk is/are less massive (making the gap less sharp) so that more dust passes through the planet-induced gap and the inner disk remains optically thick.

7. CONCLUSION

In this paper, we have used two-dimensional two-fluid simulations, a one dimensional model, and analytic arguments to study dust filtration by the tidally-induced gap outer edge. We have found that dust diffusion and the high gas velocity at the gap edge significantly lower the dust filtration efficiency. Only particles equal or larger than 0.1 mm can be filtered by the planet-induced gap

if the disk viscosity parameter is $\alpha=0.01$ and the planet mass is a few Jupiter masses. These results can be partly scaled to disks having different mass accretion rates with one dimensionless parameter T_s/α . With better understanding of the disk and gap structure, we may be able to constrain the planet mass with future multi-wavelength observations (optical/near-IR scattered images, ALMA etc.).

We have applied this dust filtration threshold (0.1 mm) to transitional disks, and by using a Monte-Carlo radiative transfer model we have shown that dust filtration alone has difficulties in explaining transitional disk observations. The same difficulty is suffered by the multiple planets scenario. One possible solution is combining dust filtration with dust growth in the inner disk, although we have also discussed other possibilities. We conclude that dust filtration is a natural consequence of gap opening in protoplanetary disks, and although it has some difficulties to explain the near-IR deficit of transitional disks (which may require additional processes such as dust growth), it has important implications for future observations.

This work was supported in part by NASA grant NNX08AI39G from the Origins of Solar Systems program, and in part by the University of Michigan. Z.Z and R.D. were also supported by NSF grant AST-0908269 and Princeton University. C. E. was supported by the National Science Foundation under Award No. 0901947. Z.Z. thanks Xuening Bai, Jim Stone, Roman Rafikov, and Steve Lubow, Ruth Murray-Clay for helpful discussion. Z.Z. also thanks Eugene Chiang for suggesting the layered accretion scenario during the International Summer Institute for Modeling in Astrophysics (ISIMA) in Beijing organized by Pascale Garaud and Doug Lin.

APPENDIX

TWO-FLUID SIMULATIONS VS. SFT APPROXIMATION VS. 1-D MODELS

We will compare the dust distribution using three different methods in this section. We expect SFT approximation should give similar results as Two-fluid simulations for particles smaller than mm, since the dust stopping time for 1 mm particles is 1/10th of the hydrodynamic time step and the SFT approximation is valid.

The comparison among two-fluid simulations, the SFT approximation, and 1-D models is shown in Figure 11 with (the right panel) and without considering dust diffusion (the left panel). A 1 M_J planet and 1 mm particles are considered and the simulations have been run to 5×10^4 yr.

As shown in Figure 11, the two-fluid simulations and the SFT approximation agree with each other quite well in both panels. For even smaller particles, the assumption of the SFT approximation will be better suited and we would expect the results to be closer to the two-fluid simulations.

The even simpler 1-D models (the long dashed curves) did a fairly good job at both the inner and outer disk beyond the gap region. The incapability of 1D models to simulate the horseshoe region is expected since the horseshoe region has intrinsically a two-dimensional flow pattern and material will be trapped inside the horseshoe region. The flow pattern there is highly non-axisymmetric with the velocity highest around the planet.

In 1-D, with the assumption that the flow is axisymmetric and the radial velocity is given by Equation 17, material in the horseshoe region will be quickly depleted. However, slightly outside the horseshoe region, even at the edge of the gap the flow is still quite axisymmetric. Considering the gap outer edge is where dust filtration takes place, the 1-D model is still capable to study dust filtration by the gap outer edge, although the dust surface density at the bottom of the gap is incorrect.

TABLE 1
MODELS

Case name	Method	Diffusion	Planet mass M_J	dust size mm	Evolution Time yr
1 M_J					
1J1mm2F	Two-fluids	No Diff	1	1	5×10^4 yr
1J1mm2FD	Two-fluids	Diff	1	1	5×10^4 yr
1J1mm	SFT approx.	No Diff	1	1	1×10^5 yr
1J0p1mm	SFT approx.	No Diff	1	0.1	2.5×10^5 yr
1J0p03mm	SFT approx.	No Diff	1	0.03	5×10^5 yr
1J1mmD	SFT approx.	Diff	1	1	1×10^5 yr
1J0p1mmD	SFT approx.	Diff	1	0.1	2.5×10^5 yr
1J0p03mmD	SFT approx.	Diff	1	0.03	5×10^5 yr
3 M_J					
3J1mm	SFT approx.	No Diff	3	1	1×10^5 yr
3J0p1mm	SFT approx.	No Diff	3	0.1	2.5×10^5 yr
3J0p03mm	SFT approx.	No Diff	3	0.03	5×10^5 yr
3J1mmD	SFT approx.	Diff	3	1	1×10^5 yr
3J0p1mmD	SFT approx.	Diff	3	0.1	2.5×10^5 yr
3J0p03mmD	SFT approx.	Diff	3	0.03	5×10^5 yr
6 M_J					
1J1mm	SFT approx.	No Diff	6	1	1×10^9 yr
1J0p1mm	SFT approx.	No Diff	6	0.1	2.5×10^5 yr
1J0p03mm	SFT approx.	No Diff	6	0.03	5×10^5 yr
1J1mmD	SFT approx.	Diff	6	1	1×10^5 yr
1J0p1mmD	SFT approx.	Diff	6	0.1	2.5×10^5 yr
1J0p03mmD	SFT approx.	Diff	6	0.03	5×10^5 yr

REFERENCES

- Andrews, S. M., Wilner, D. J., Hughes, A. M., Qi, C., & Dullemond, C. P. 2009, *ApJ*, 700, 1502
- Andrews, S. M., Wilner, D. J., Espaillat, C., et al. 2011, *ApJ*, 732, 42
- Andrews, S. M., Wilner, D. J., Hughes, A. M., et al. 2012, *ApJ*, 744, 162
- Alexander, R. D., & Armitage, P. J. 2007, *MNRAS*, 375, 500
- Birnstiel, T., Klahr, H., & Ercolano, B. 2012, *arXiv:1201.5781*
- Birnstiel, T., Ormel, C. W., & Dullemond, C. P. 2011, *A&A*, 525, A11
- Brown, J. M., et al. 2007, *ApJ*, 664, L107
- Brown, J. M., Blake, G. A., Qi, C., Dullemond, C. P., Wilner, D. J., & Williams, J. P. 2009, *ApJ*, 704, 496
- Calvet, N., D'Alessio, P., Hartmann, L., Wilner, D., Walsh, A., & Sitko, M. 2002, *ApJ*, 568, 1008
- Calvet, N., et al. 2005, *ApJ*, 630, L185
- Carballido, A., Bai, X.-N., & Cuzzi, J. N. 2011, *MNRAS*, 415, 93
- Chiang, E., & Murray-Clay, R. 2007, *Nature Physics*, 3, 604
- Crida, A., Morbidelli, A., & Masset, F. 2007, *A&A*, 461, 1173
- D'Alessio, P., Calvet, N., & Hartmann, L. 2001, *ApJ*, 553, 321
- D'Alessio, P., et al. 2005, *ApJ*, 621, 461
- Dodson-Robinson, S. E., & Salyk, C. 2011, *ApJ*, 738, 131
- Dullemond, C. P., & Dominik, C. 2005, *A&A*, 434, 971
- Dominik, C., & Dullemond, C. P. 2008, *A&A*, 491, 663
- Dominik, C., & Dullemond, C. P. 2011, *A&A*, 531, A101
- Dong, R., Rafikov, R., Zhu, Z., et al. 2012, *ApJ*, 750, 161
- Espaillat, C., Calvet, N., D'Alessio, P., Hernández, J., Qi, C., Hartmann, L., Furlan, E., & Watson, D. M. 2007, *ApJ*, 670, L135
- Espaillat, C., Calvet, N., Luhman, K. L., Muzerolle, J., & D'Alessio, P. 2008, *ApJ*, 682, L125
- Espaillat, C., D'Alessio, P., Hernández, J., et al. 2010, *ApJ*, 717, 441
- Espaillat, C., Ingleby, L., Hernandez, J., et al. 2012, *arXiv:1201.1518*
- Fouchet, L., Maddison, S. T., Gonzalez, J.-F., & Murray, J. R. 2007, *A&A*, 474, 1037
- Furlan, E., Hartmann, L., Calvet, N., et al. 2006, *ApJS*, 165, 568
- Gullbring, E., Hartmann, L., Briceno, C., & Calvet, N. 1998, *ApJ*, 492, 323
- Hartmann, L., Calvet, N., Gullbring, E., & D'Alessio, P. 1998, *ApJ*, 495, 385
- Hughes, A. M., et al. 2009, *ApJ*, 698, 131
- Isella, A., Perez, L. M., & Carpenter, J. M. 2012, *arXiv:1201.1001*
- Johansen, A., & Klahr, H. 2005, *ApJ*, 634, 1353
- Kim, S.-H., Martin, P. G., & Hendry, P. D. 1994, *ApJ*, 422, 164
- Marsh, K. A., & Mahoney, M. J. 1992, *ApJ*, 395, L115
- Masset, F. 2000, *A&AS*, 141, 165
- Mathis, J. S., Rumpl, W., & Nordsieck, K. H. 1977, *ApJ*, 217, 425
- Najita, J. R., Strom, S. E., & Muzerolle, J. 2007, *MNRAS*, 378, 369
- Paardekooper, S.-J., & Mellema, G. 2006, *A&A*, 453, 1129
- Pierens, A., & Nelson, R. P. 2008, *A&A*, 482, 333
- Piétu, V., Dutrey, A., Guilloteau, S., Chapillon, E., & Pety, J. 2006, *A&A*, 460, L43
- Rice, W. K. M., Armitage, P. J., Wood, K., & Lodato, G. 2006, *MNRAS*, 373, 1619
- Robitaille, T. P., Whitney, B. A., Indebetouw, R., Wood, K., & Denzmore, P. 2006, *ApJS*, 167, 256
- Schneider, G., Wood, K., Silverstone, M. D., Hines, D. C., Koerner, D. W., Whitney, B. A., Bjorkman, J. E., & Lowrance, P. J. 2003, *AJ*, 125, 1467
- Salyk, C., Blake, G. A., Boogert, A. C. A., & Brown, J. M. 2007, *ApJ*, 655, L105
- Stone, J. M., & Norman, M. L. 1992, *ApJS*, 80, 753
- Strom, K. M., Strom, S. E., Edwards, S., Cabrit, S., & Skrutskie, M. F. 1989, *AJ*, 97, 1451
- Takeuchi, T., & Lin, D. N. C. 2002, *ApJ*, 581, 1344
- Younis, A. N., & Lithwick, Y. 2007, *ICARUS*, 192, 588
- Ward, W. R. 2009, *Lunar and Planetary Institute Science Conference Abstracts*, 40, 1477
- Weidenschilling, S. J. 1977, *MNRAS*, 180, 57
- Whipple, F. L. 1972, *From Plasma to Planet*, 211
- Whitney, B. A., Wood, K., Bjorkman, J. E., & Wolff, M. J. 2003, *ApJ*, 591, 1049
- Whitney, B. A., Wood, K., Bjorkman, J. E., & Cohen, M. 2003, *ApJ*, 598, 1079
- Whitney, B. A., et al., 2012, in preparation
- Wood, K., Wolff, M. J., Bjorkman, J. E., & Whitney, B. 2002, *ApJ*, 564, 887
- Zhu, Z., Nelson, R. P., Hartmann, L., Espaillat, C., & Calvet, N. 2011, *ApJ*, 729, 47

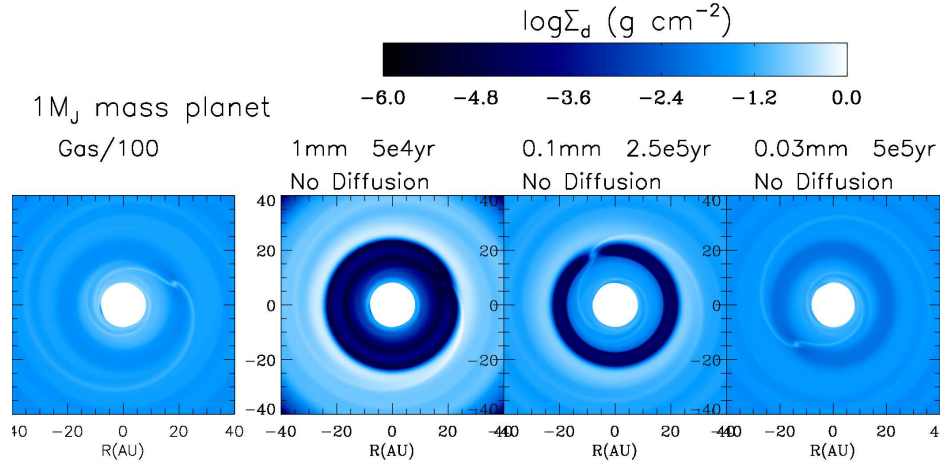


FIG. 1.— The disk gas (left panel) and different sized dust (right panels) surface density contours if a $1 M_J$ planet is at 20 AU. The gas surface density is divided by 100 to scale with the dust surface densities. Three different sized dust has been shown in the right panels. Dust diffusion has been turned off in these simulations. For 1 mm particles, the contour shows the surface density at 5×10^4 yr, which is longer than the dust drift timescale. For 0.1 mm particles, the surface density shown is at 2.5×10^5 yr, which is even longer than the disk viscous timescale at 20 AU. For 0.03 mm particles, the surface density shown is at 5×10^5 yr. Clearly, 1 mm particles are filtered by the planet-induced gap. Particles smaller than 1 mm can penetrate the gap freely.

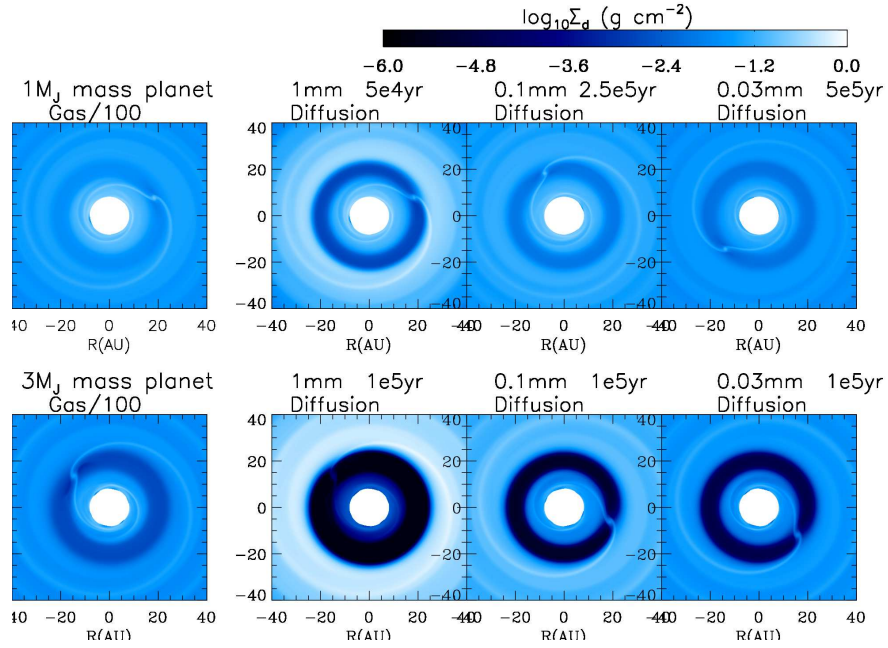


FIG. 2.— Upper panels: similar to Figure 1 but with dust diffusion due to disk turbulence included. Clearly dust diffusion leads to less efficient dust filtration. Bottom panels: Similar to the upper panel but with a $3 M_J$ planet in the disk. The inner disk for 1 mm dust is depleted, while for 0.1 mm and 0.03 mm dust the dust inner disk is still present. Since the gaps in the bottom panels are very deep, the color bar is from -10 to 0 for the 1 mm case, -7 to 0 for the 0.1 mm case, and -6 to 0 for the 0.03 mm case.

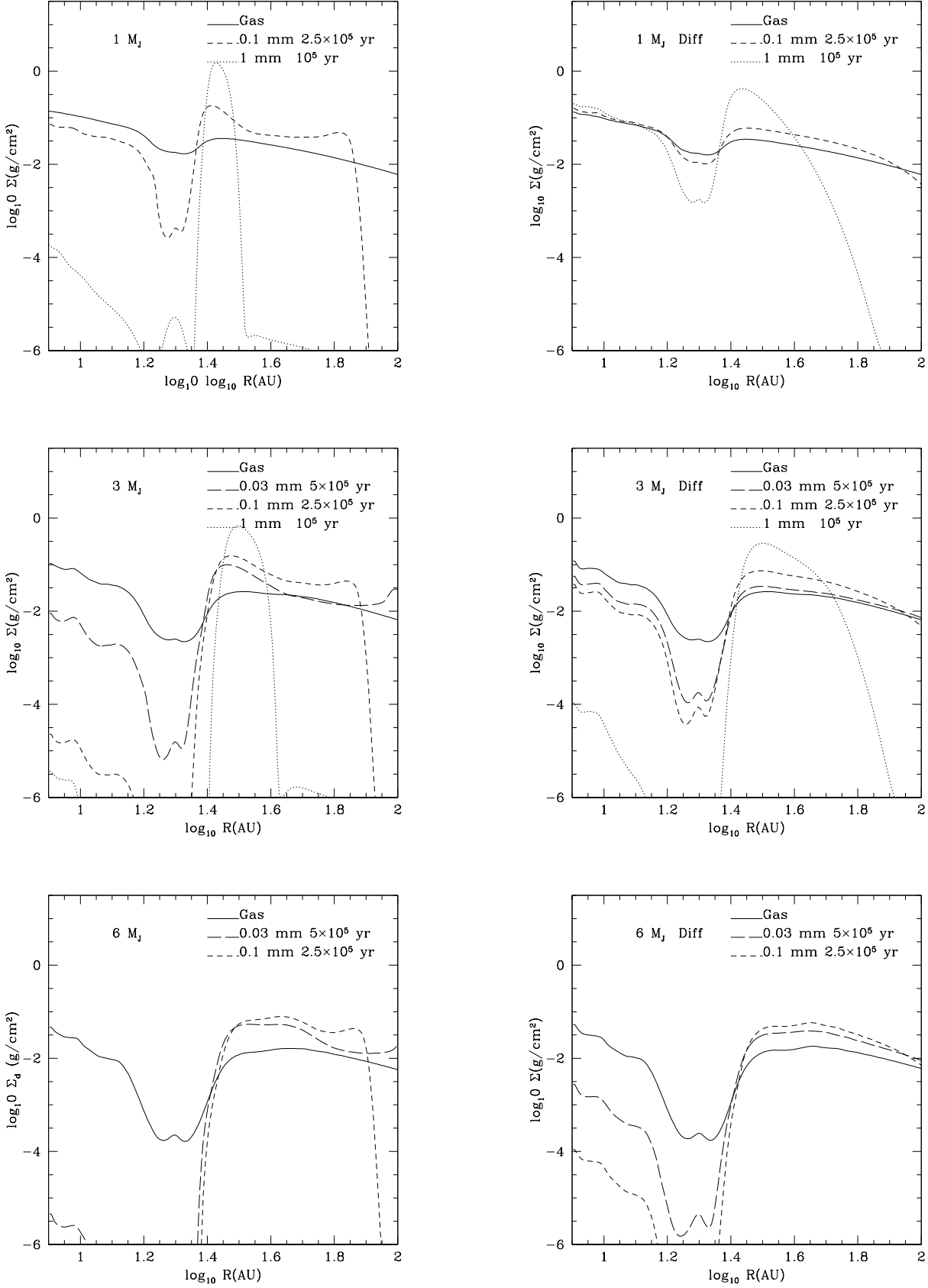


FIG. 3.— The azimuthal averaged gas (solid curves) and dust surface densities (1 mm: dotted curves, 0.1 mm: dashed curves, 0.03 mm: long dashed curves) if the planet is at 20 AU with different masses ($1 M_J$ upper panels, $3 M_J$ middle panels, and $6 M_J$ lower panels). The left panels are without dust diffusion, while the right panels are with dust diffusion considered. 1 mm particles are shown at 10^4 yrs which is longer than its radial drift timescale, while 0.1 mm and 0.01 mm particles are shown at 2.5×10^5 yrs and 5×10^5 yrs since their drift timescales are longer. The gas surface densities are divided by 100 to scale with the dust surface densities.

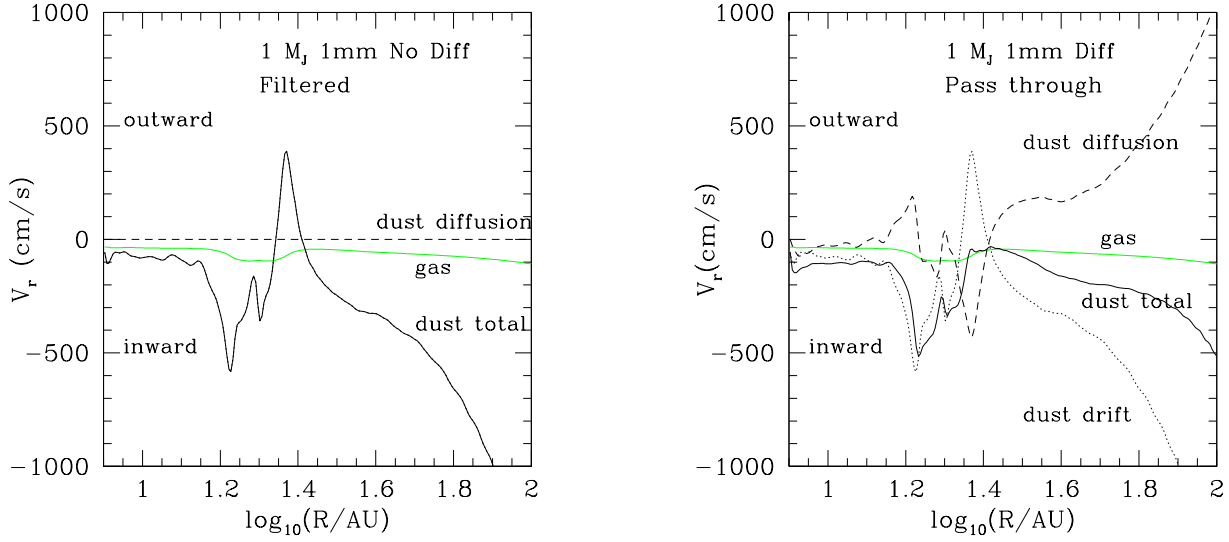


FIG. 4.— The 1 mm dust radial drift velocity from 1-D models with (right panel) and without (left panel) diffusion considered. The green curves are the gas radial velocity. The solid curves are the total dust radial velocity, among which the dotted curves are the component due to the pressure gradient and gas velocity, and the dashed curves are the component due to dust diffusion. Thus, if dust diffusion is ignored, 1mm particles can be trapped by the outer edge of the gap opened by a $1 M_J$ planet (the dust velocity is positive at the gap outer edge in the left panel). But with dust diffusion, 1mm particles can pass through the gap (the total dust velocity is negative at the gap outer edge in the right panel).

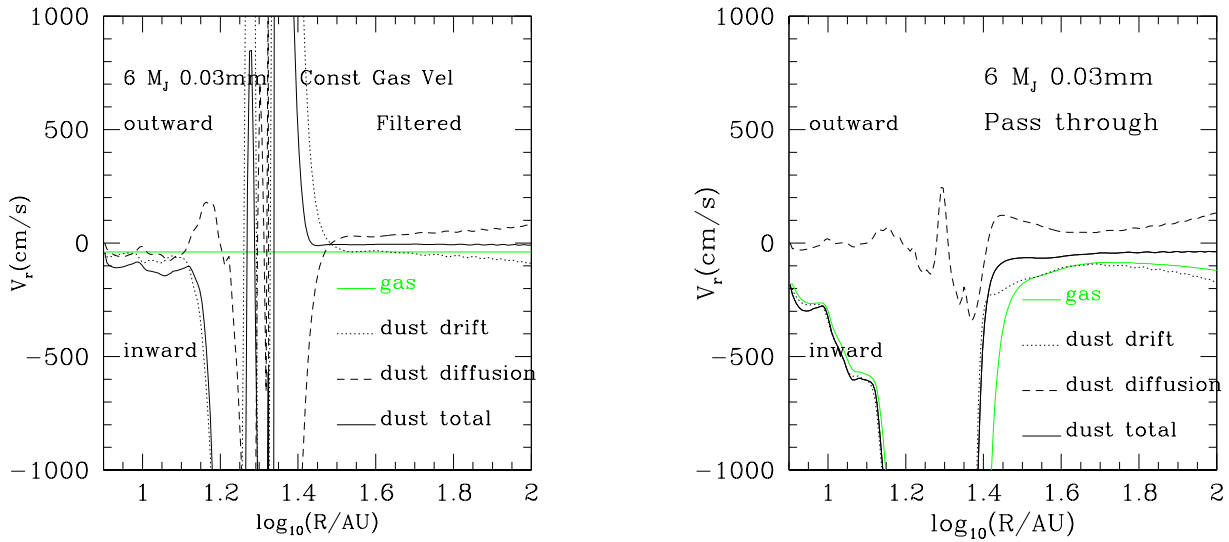


FIG. 5.— The 0.03 mm dust radial drift velocities from 1-D models with a $6 M_J$ planet at 20 AU. Dust diffusion has been considered in both cases. The simulation in the left panel assumes the gas velocity is constant across the planet-induced gap, while the simulation in the right panel assumes the gas mass accretion rate is constant across the gap. The green curves are the gas radial velocity. The solid curves are the dust radial velocity, among which the dotted curves are the component due to the pressure gradient and gas velocity, and the dashed curves are the component due to dust diffusion (the significant velocity variation inside the gap in the left panel is due to the small structures at the corotation region and the incorrect 1-D treatment there, see Appendix). Thus, if the amplification of the gas velocity at the gap outer edge is ignored, 0.03mm particles can be trapped by the gap edge (the dust velocity, solid curve, is positive at the gap outer edge in the left panel). But with the amplification of the gas velocity is considered, 0.03 mm particles can pass through the planet-induced gap (the dust velocity is negative at the gap outer edge in the right panel).

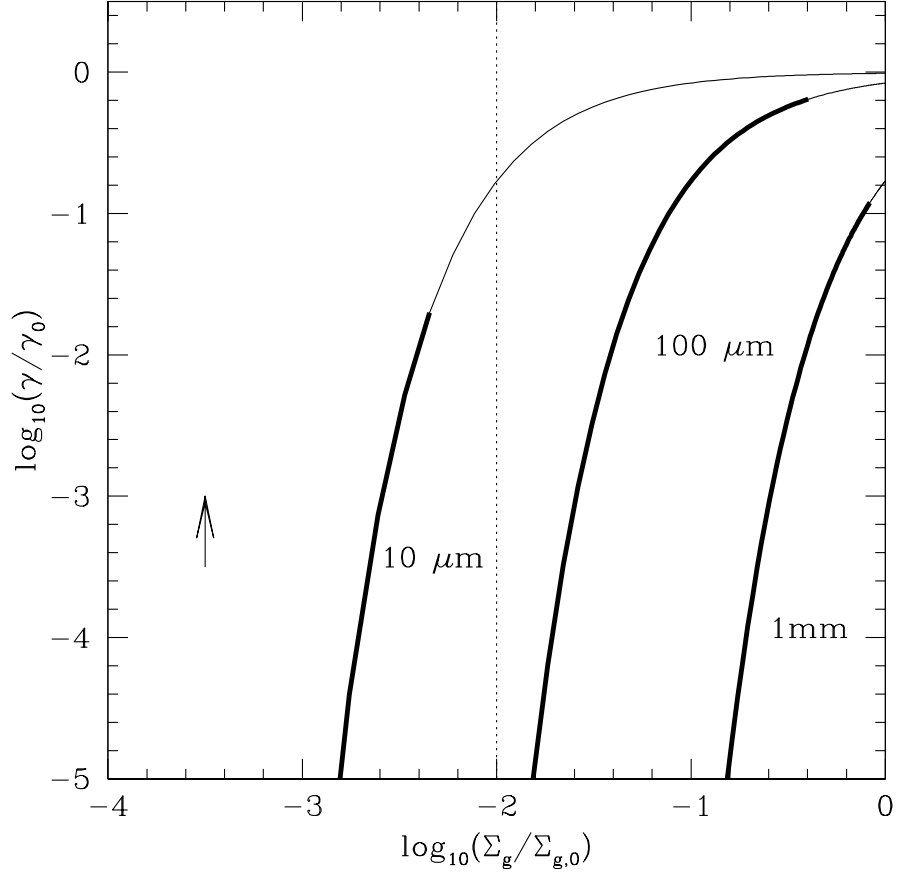


FIG. 6.— The dust depletion factor due to dust filtration (the depletion of the dust to gas mass ratio with respect to a full disk) with respect to the planet-induced gap depth for different sized particles. Dust diffusion is considered. The thick solid curves are the exact value while the thin curves are the lower limit since the gas velocity amplification is important there. The gap depth of 10^{-2} which is opened by a planet with a few Jupiter mass in a $\alpha=0.01$ disk is also labeled. The arrow indicates the dust depletion factor 1000, which is used by us to determine if dust will be filtered.

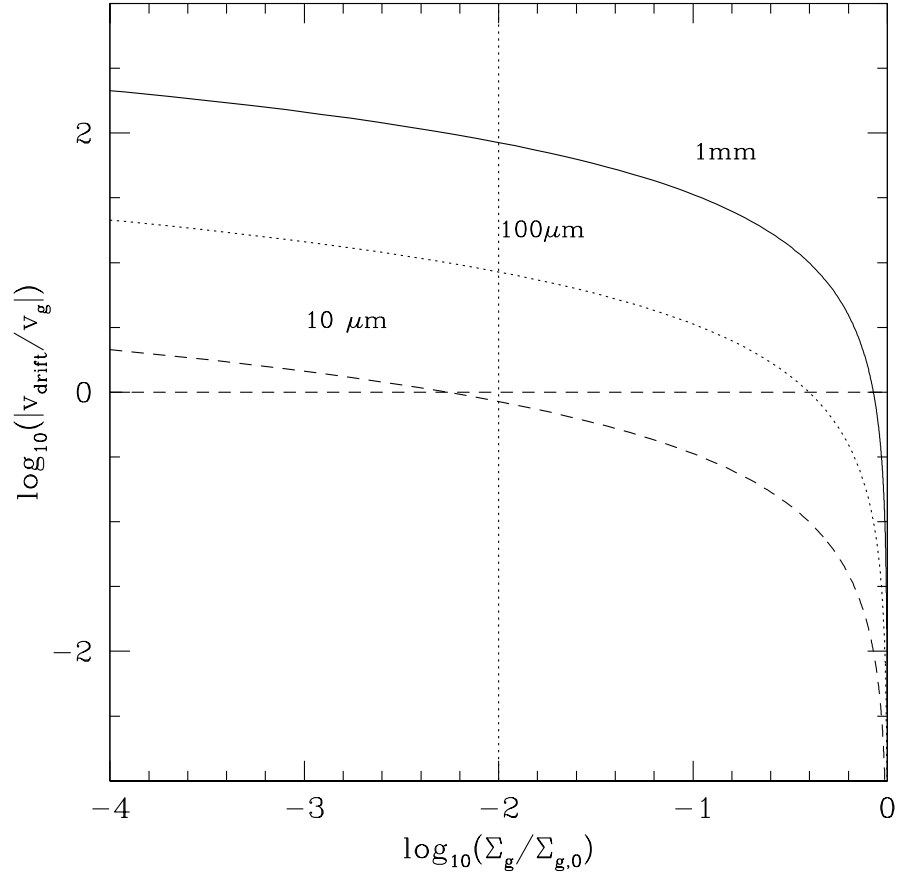


FIG. 7.— The relationship between the ratio of the dust drift velocity over the gas velocity and the gap depth. Dust diffusion is ignored in this calculation. If the ratio is larger than 1, particles will be trapped. Otherwise, particles will be carried inwards through the planet-induced gap by the gas. Different sized particles (1 mm, $100\mu\text{m}$, and $10\mu\text{m}$) have been considered. Note that the gas velocities are amplified in the gap. The gap depth of 10^{-2} which is opened by a planet with a few Jupiter mass in a $\alpha=0.01$ disk is also labeled.

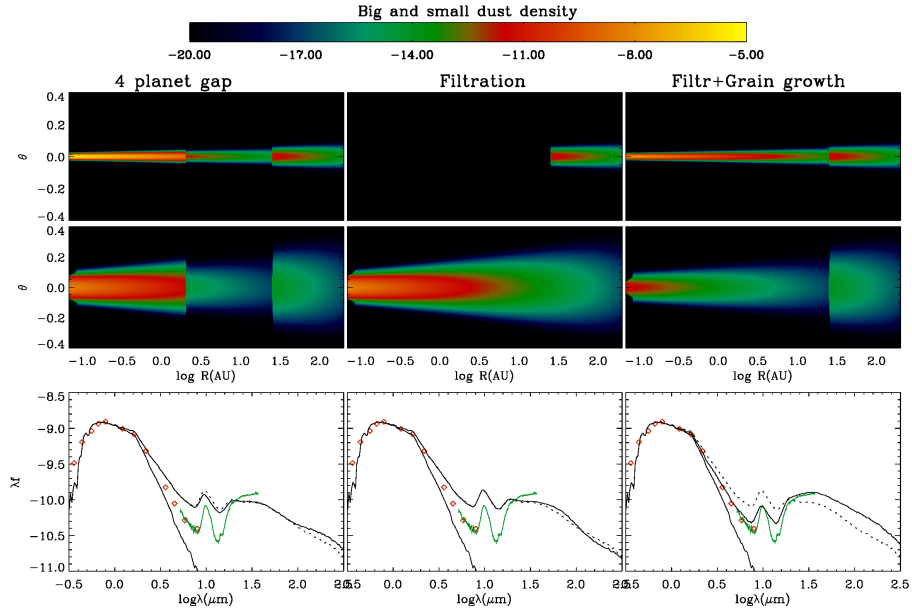


FIG. 8.— Various scenarios to explain transitional disks GM Aur. 1) a wide gap opened by multiple planets (left panels); 2) a deep gap opened by one planet which can filter large dust particles (middle panels); and 3) After big particles are filtered by the gap, small particles can grow (right panels). The upper panels show the dust density distribution for large particles ($\geq 10 \mu\text{m}$) in the disk (big particles are totally filtered in the second scenario and some new big particles are generated in the third scenario), while the middle panels show the dust density distribution for small particles ($\leq 10 \mu\text{m}$) in the disk (small dust is continuous in the second scenario). The lower panels show the SED from these models. The dotted curve is the SED from a full disk. Photometric (red, open symbols) and IRS data (green) for GM Aur are from Espaillat et al. 2011; refer to that work for more details. As clearly shown, either gap opening by multiple planets or dust filtration (left and right panels) has little effect on the SED compared with a full disk (solid curves overlap with the dotted curves). This is because small dust particles in the inner disk ($< 1 \text{ AU}$, which produce most of the optical and IR flux) still have similar abundance as the full disk model. But dust filtration plus dust growth can explain transitional disk SED, since small dust particles in the inner disk ($< 1 \text{ AU}$) are depleted significantly in this scenario.

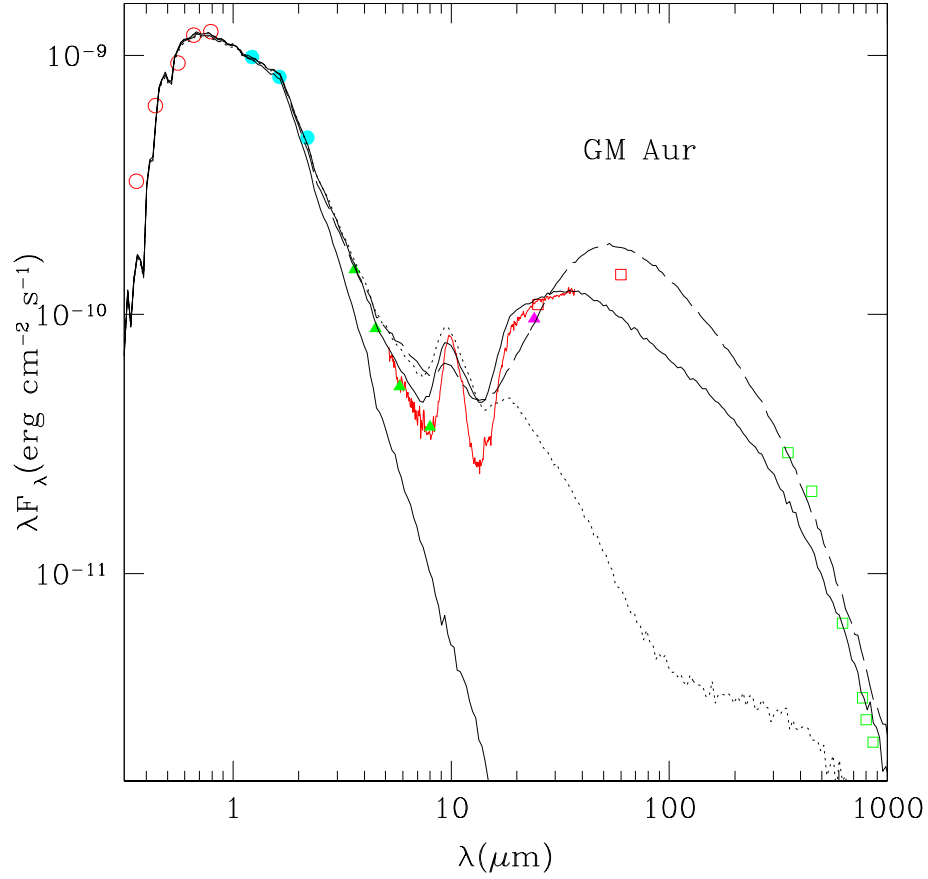


FIG. 9.— The photometry and spectrum for GM Aur (colored dots and curves) and three model SEDs. The solid black curve is from our best fit model as in the right panels of Fig. 8 considering both dust filtration and dust growth. The dotted curve is from the dust filtration only model (similar to the middle panels of Fig. 8) but with small/large dust ratio 10^{-5} at the outer disk (we call this the extreme dust filtration case). This model can reproduce the near-IR flux since, after big particles are filtered by the planet-induced gap, it basically has the same amount of small dust in the inner disk as our best fit model. However due to the lack of small dust at the outer disk, the outer disk is quite optically thin with big particles settle to the midplane (20% thickness) and produces very little mid-IR flux. The dashed curve is similar to the dotted curve, but the big dust at the outer disk do not settle and have the same thickness as the gaseous disk.

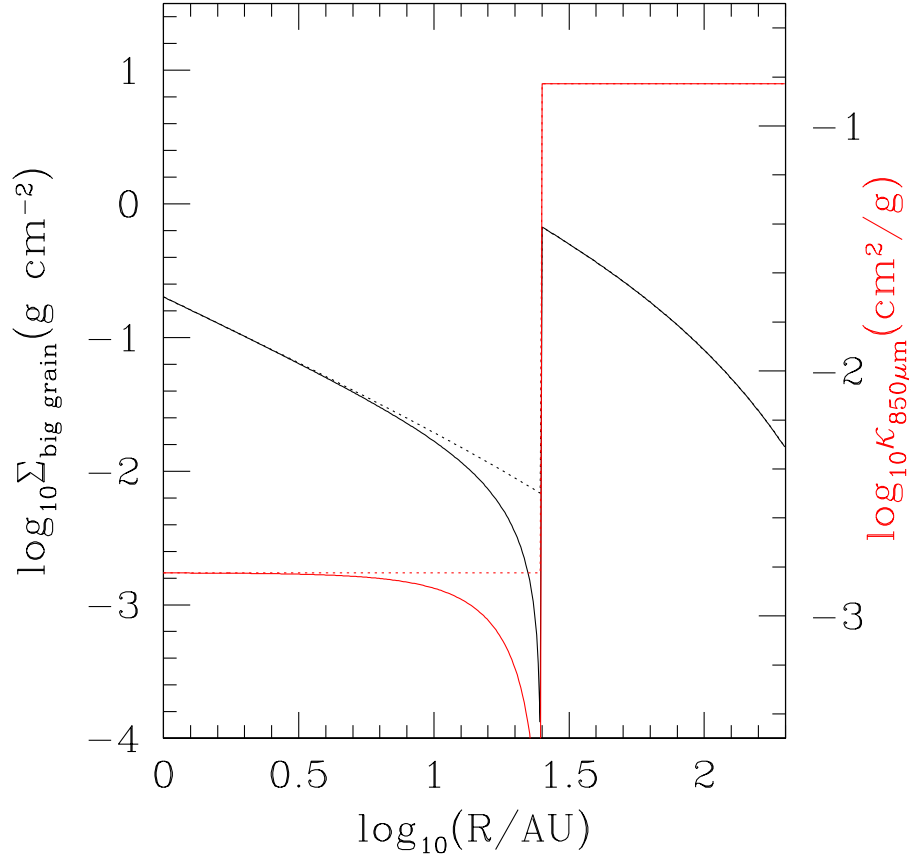


FIG. 10.— The big grain ($\gtrsim 10 \mu\text{m}$) surface density in the filtration+grain growth scenario (the right panels of Figure 8), and the $850 \mu\text{m}$ opacity (the red curves). The opacity is calculated by dividing the total optical depth at $850 \mu\text{m}$ over the gas surface density (which is the same as our full disk model having continuous increasing gas surface density inwards). The dotted curves are from the model presented in the right panels of Figure 8, where grains are assumed to grow instantaneously after they pass through the gap. This is for numerical convenience. The solid curves should be more close to a real protoplanetary disk, where grain growth is a gradual process. As shown, the big grains deplete significantly across the gap at 20 AU where they are filtered. And thus the submm opacity decreases significantly too. The exact value is only for our particular model. But the trend that the submm opacity decreases at the gap edge and then increases inwards is a signature for filtration+grain growth scenario, which can be tested by ALMA.

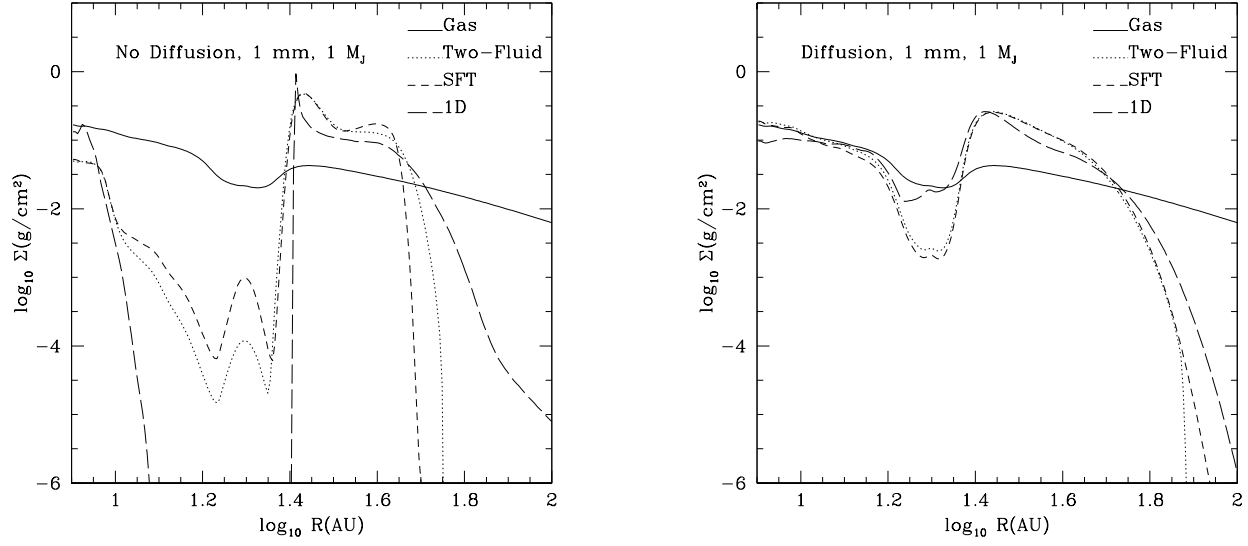


FIG. 11.— The azimuthal averaged gas (solid curve) and 1mm dust surface densities with(right panel) and without (left panel) dust diffusion at $t=5 \times 10^4$ yr. The gas surface density is divided by 100 to scale with the dust surface density. Results from various methods are compared. The dotted curves are from 2-D two-fluid simulations, while the short dashed curves are from the SFT approximation. The long dashed curves are from the simplified 1-D simulations. These methods agree with each other outside the gap or even at the outer edge of the gap, suggesting they give consistent results regarding dust filtration. But 1-D simulations failed to reproduce the horseshoe ring around the planet in the left panel.